OFFICE OF NAVAL RESEARCH

Contract N00014-84-G-0201

Task No. 0051-865

Technical Report #30

Perchlorinated Phthalocyanines: Spectroscopic Properties and Surface Electrochemistry

By

M.N. Golovin, P. Seymour, K. Jayaraj, Y. Fu and A.B.P. Lever*

in

Inorganic Chemistry

York University
Department of Chemistry, 4700 Keele St., North York
Ontario, Canada M3J 1P3

SECURITY CLASSIFICATION OF THIS PAGE

REPORT DOCUMENTATION PAGE

1a. REPORT SECURITY CLASSIFICATION	1b. RESTRICTIVE MARKINGS
2a. SECURITY CLASSIFICATION AUTHORITY: Unclassified	3. DISTRIBUTION/AVAILABILITY OF REPORT: As it appears on the report
2b. DECLASSIFICATION/DOWNGRADING SCHEDULE	
4. PERFORMING ORGANIZATION REPORT NUMBER(S): Report # 30	5. MONITORING ORGANIZATION REPORT NUMBER(S)
6a. NAME OF PERFORMING ORGANIZATION: A.B.P. Lever, York University Chemistry Department; 6b. OFFICE SYMBOL (If applicable)	7a. NAME OF MONITORING ORGANIZATION: Office of Naval Research
6c. ADDRESS (City, State, and ZIP Code): 4700 Keele St., North York, Ontario M3J 1P3 Canada	7b. ADDRESS (City, State, and ZIP Code): Chemistry Division, 800 N. Quincy Street, Arlington, VA 22217 U.S.A.
8a. NAME OF FUNDING/SPONSORING ORGANIZATION; 8b. OFFICE SYMBOL (If applicable)	9. PROCUREMENT INSTRUMENT IDENTIFICATION NUMBER: N00014-84-G-0201
8c. ADDRESS (City, State, and ZIP Code)	10. SOURCE OF FUNDING NUMBERS: PROGRAM ELEMENT NO. / PROJECT NO. / TASK NO / WORK UNIT ACCESSION NO

11. TITLE (Include Security Classification)

Perchlorinated Phthalocyanines: Spectroscopic Properties and Surface Electrochemistry

12. PERSONAL AUTHOR(S)

M.N. Golovin, P. Seymour, K. Jayaraj, Y. Fu and A.B.P. Lever

13a. TYPE OF REPORT	13b. TIME COVERED	14. DATE OF REPORT (Year, Month, Day)	15. PAGE COUNT
Technical	FROM Aug. 89 TO Aug. 90	March 1, 1990	46

16. SUPPLEMENTARY NOTATION

17 COSATI CODES		
FIELD	GROUP	SUB-GROUP

18. SUBJECT TERMS (Continue on reverse if necessary and identify by block number)

Phthalocyanine, Electrochemistry Surfaces, Electronic Spectra

19. ABSTRACT (Continue on reverse if necessary and identify by block number)

The electronic spectroscopic data for zinc, cobalt and iron perchlorinated phthalocyanines in several oxidation states are discussed. The magnetic properties of the iron(II) and cobalt(II) derivatives from ambient temperature to 5 K are reported. The electrochemical behaviour of these three species is reported in solution and as surfaces on highly oriented pyrolytic graphite. The pH dependence of the surface data is analysed in detail. The first clearly defined reduction process corresponds with $M(I)[Cl_{16}Pc(-2)]^{-}/M(I)[Cl_{16}Pc(-3)]^{2-}$ for M = Co,Fe. The iron and cobalt species $M(II)Pc(-2)/[M(I)Pc(-2)]^{+}$ redox process are broad or ill-defined on the surface, and absent from solution. The $Fe(III)[Cl_{16}Pc(-2)]^{+}/Fe(II)[Cl_{16}Pc(-2)]$ redox process has atypical pH dependence. The data are explained in terms of the acceptor nature of the chlorine substitution. Oxygen reduction data, catalysed by these species, are also reported.

20. DISTRIBUTION/AVAILABILITY OF ABSTRACT	21. ABSTRACT SECURITY CLASSIFICATION
☒ UNCLASSIFIED/UNLIMITED ☐ SAME AS RPT ☐ DTIC USERS	Unclassified/unlimited
22a. NAME OF RESPONSIBLE INDIVIDUAL: Dr. Robert K. Grasselli	22b. TELEPHONE (Include Area Code) / 22c. OFFICE SYMBOL

DD FORM 1473, 84 MAR — 83 APR edition may be used until exhausted. All other editions are obsolete.

SECURITY CLASSIFICATION OF THIS PAGE

DL/1113/89/1

TECHNICAL REPORT DISTRIBUTION LIST, GENERAL

	No. Copies
Office of Naval Research Chemistry Division, Code 1113 800 North Quincy Street Arlington, VA 22217-5000	3
Commanding Officer Naval Weapons Support Center Attn: Dr. Bernard E. Douda Crane, IN 47522-5050	1
Dr. Richard W. Drisko Naval Civil Engineering Laboratory Code L52 Port Hueneme, California 93043	1
Defense Technical Information Center Building 5, Cameron Station Alexandria, Virginia 22314	2 high quality
David Taylor Research Center Dr. Eugene C. Fischer Annapolis, MD 21402-5067	1
Dr. James S. Murday Chemistry Division, Code 6100 Naval Research Laboratory Washington, D.C. 20375-5000	1
Dr. Ronald L. Atkins Chemistry Division (Code 385) Naval Weapons Center China Lake, CA 93555-6001	1
Chief of Naval Research Special Assistant for Marine Corps Matters Code 00MC 800 North Quincy Street Arlington, VA 22217-5000	1
Dr. Bernadette Eichinger Naval Ship Systems Engineering Station Code 053 Philadelphia Naval Base Philadelphia, PA 19112	1
Dr. Sachio Yamamoto Naval Ocean Systems Center Code 52 San Diego, CA 92152-5000	1
David Taylor Research Center Dr. Harold H. Singerman Annapolis, MD 21402-5067 ATTN: Code 283	1

ONR Electrochemical Sciences Program
Abstracts Distribution List (9/89)

Dr. Henry White
Department of Chemical Engineering and
Materials Science
421 Washington Ave., SE
Minneapolis, MN 55455
(612) 625-3043
400o027yip

Dr. A. B. P. Lever
Department of Chemistry
York University
4700 Keele Street
North York, Ontario M3J 1P3
(416) 736-2100 Ext. 2309
4131025

Dr. Mark Wrighton
Department of Chemistry
Massachusetts Institute of Technology
Cambridge, MA 02139
(617) 253-1597
4131027

Dr. Michael Weaver
Department of Chemistry
Purdue University
West Lafayette, IN 49707
(317) 494-5466
4133001

Dr. Lesser Blum
Department of Physics
University of Puerto Rico
Rio Piedras, PUERTO RICO 00931
(809) 763-3390
4133002

Dr. R. David Rauh
EIC Laboratories, Inc.
111 Downey Street
Norwood, MA 02062
(617) 769-9450
4133003

Dr. Rudolph Marcus
Division of Chemistry and Chemical Engineering
California Institute of Technology
Pasadena, CA 91125
(818) 356-6566
4133004

Dr. Donald Sandstrom
Boeing Aerospace Company
P.O. Box 3999, M/S 87-08
Seattle, WA 98124-2499
(206) 773-2272
4133007

Dr. Ernest Yeager
Director, Case Center for
Electrochemical Sciences
Case Western Reserve University
Cleveland, OH 44106
(216) 368-3626
4133008

Dr. S. Pons
Department of Chemistry
University of Utah
Salt Lake City, UT 84112
(801) 581-4760
4133010

Dr. Michael R. Philpott
IBM Research Division
Almaden Research Center
650 Harry Road
San Jose, CA 95120-6099
(408) 927-2410
4133011

Dr. Ulrich Stimming
Department of Chemical Engineering
and Applied Chemistry
Columbia University
New York, NY 10027
(212) 280-8755
4133014

Dr. Royce W. Murray
Department of Chemistry
University of North Carolina at Chapel Hill
Chapel Hill, NC 27514
(919) 962-6295
4133015

Dr. D. E. Irish
Department of Chemistry
University of Waterloo
Waterloo, Ontario, CANADA N21 3G1
(519) 885-1211 ext. 2500
4133016

Dr. Daniel Buttry
Department of Chemistry
University of Wyoming
Laramie, WY 82071
(307) 766-6677
4133019

Dr. W. R. Fawcett
Department of Chemistry
University of California, Davis
Davis, CA 95616
(916) 752-1105
4133020

Dr. Joseph Hupp
Department of Chemistry
Northwestern University
Evanston, IL 60208
(312) 491-3504
4133025

Dr. Andrew Ewing
Department of Chemistry
152 Davey Laboratory
Pennsylvania State University
University Park, PA 16802
(814) 863-4653
4133030

Dr. Martin Fleischmann
Department of Chemistry
The University
Southampton SO9 5NH
UNITED KINGDOM
0703-559122
4134001

Dr. Allen Bard
Department of Chemistry
The University of Texas at Austin
Austin, TX 78712-1167
(512) 471-3761
413a002

Dr. Joel Harris
Department of Chemistry
University of Utah
Salt Lake City, UT 84112
(801) 581-3585
413a005

Dr. J. O. Thomas
Institute of Chemistry, Box 531
University of Uppsala
S-751 21 Uppsala
SWEDEN
413d003

Dr. Gregory Farrington
Laboratory for Research on the
Structure of Matter
3231 Walnut Street
Philadelphia, PA 19104-6202
(215) 898-6642
413d003

Dr. Charles Martin
Department of Chemistry
Texas A&M University
College Station, TX 77843
(409) 845-7638
413d005

Dr. C. A. Angell
Arizona State University
Department of Chemistry
Tempe, AZ 85287
(602) 965-7217
413d007

Dr. Martha Greenblatt
Department of Chemistry
Rutgers University
Piscataway, NJ 08854
(201) 932-3277
413d008

Dr. Bruce Dunn
Departement of Materials Science and Engineering
University of California, Los Angeles
Los Angeles, CA 90024
(213) 825-1519
413d011

Dr. James Brophy
Department of Physics
University of Utah
Salt Lake City, UT 84112
(801) 581-7236
413d015

Dr. Richard Pollard
Department of Chemical Engineering
University of Houston, University Park
4800 Calhoun, Houston, TX 77004
(713) 749-2414
413d016

Dr. Nathan S. Lewis
Division of Chemistry and Chemical Engineering
California Institute of Technology
Pasadena, CA 91125
(415) 723-4574
413d017

Dr. Hector Abruña
Department of Chemistry
Cornell University
Ithaca, NY 14853
(607) 256-4720
413d018

Dr. Adam Heller
Department of Chemical Engineering
The University of Texas at Austin
Austin, TX 78712-1062
(512) 471-5238
413h007

Dr. Petr Vanýsek
Department of Chemistry
Northern Illinois University
Dekalb, IL 60115
(815) 753-6876
413k001

Dr. George Wilson
Department of Chemistry
University of Kansas
Lawrence, KS 66045
(913) 864-4673
413k002

Dr. H. Gilbert Smith
EG&G Mason Research Institute
57 Union Street
Worcester, MA 01608
(617) 791-0931
413k003

Perchlorinated Phthalocyanines: Spectroscopic Properties and Surface Electrochemistry.

M. Neal Golovin, Penny Seymour, Karupiah Jayaraj, YanSong Fu, and A.B.P. Lever*

Abstract

The electronic spectroscopic data for zinc, cobalt and iron perchlorinated phthalocyanines in several oxidation states are discussed. The magnetic properties of the iron(II) and cobalt(II) derivatives from ambient temperature to 5 K are reported. The electrochemical behaviour of these three species is reported in solution and as surfaces on highly oriented pyrolytic graphite. The pH dependence of the surface data is analysed in detail. The first clearly defined reduction process corresponds with $M(I)[Cl_{16}Pc(-2)]^-$ / $M(I)[Cl_{16}Pc(-3)]^{2-}$ for M = Co,Fe. The iron and cobalt species' $M(II)Pc(-2)/[M(I)Pc(-2)]^-$ redox process are broad or ill-defined on the surface, and absent from solution. The $Fe(III)[Cl_{16}Pc(-2)]^+$ /$Fe(II)[Cl_{16}Pc(-2)]$ redox process has atypical pH dependence. The data are explained in terms of the acceptor nature of the chlorine substitution. Oxygen reduction data, catalysed by these species, are also reported.

Introduction

Perchlorinated phthalocyanine (scheme I) derivatives have been reported in the literature[1,2] but their chemical and physical properties have not been investigated in any depth. We report here our results on the preparation, spectroscopic and electrochemical (surface and solution) properties of the iron, cobalt and zinc derivatives, M[Cl_{16}Pc(-2)]. The electrocatalysis of the cathodic reduction of O_2 at M[Cl_{16}Pc(-2)] modified graphite electrodes has also been studied here. The electron acceptor character of the substituents imposes some well defined changes on the properties of these complexes relative to unsubstituted or electron donor substituted species. These perchlorinated species are under intense study industrially as optical recording medium substrates, infrared light detectors, reprographic photoreceptors etc., as witnessed by the existence of many patents.[3-12]

Experimental

The solvents used in the syntheses, namely, acetone, methylene chloride, and N,N-dimethyl formamide (DMF) were all reagent grade, and used as supplied.

The complexes were prepared by a template reaction[1,2] involving the reaction of tetrachlorophthalic anhydride, urea, ammonium molybdate, and the appropriate metal salt ($FeCl_2 \cdot 4H_2O$ for Fe[Cl_{16}Pc(-2)] (1) and $Zn(C_2H_3O_2) \cdot 2H_2O$ for Zn[Cl_{16}Pc(-2)] (2)), heated in nitrobenzene to 200 °C for four to eight hrs. After cooling, the solutions were diluted with ethanol, boiled for ten minutes and filtered hot. These products were purified further by refluxing in 1% aqueous HCl and then 1% aqueous NaOH. The filtered products were then dissolved in conc. H_2SO_4, filtered, and recovered by pouring this filtrate over ice. The zinc product was further purified by recystallisation from DMF. The iron product was further purified by extraction with methylene chloride and acetone (the pure product remaining in the soxhlet thimble). Both products analysed satisfactorily (Anal.

C,N).

The cobalt complex, Co[Cl_{16}Pc(-2)] (3) was prepared in a similar manner using $CoCl_2 \cdot 4H_2O$ and tetrachlorophthalonitrile instead of the anhydride and urea. After the final extraction with methylene chloride, the cobalt derivative was purified by extraction with DMF leading to dissolution and recovery of a DMF mono-adduct. (Anal. C,H,N).

Magnetic Data Data were collected using the Faraday method and equipment previously described.[13] We are indebted to Prof.L.K.Thompson, Memorial University, for the collection of these data. All data are presented in the format:- temperature K, molar susceptibility in $cm^3 mol^{-1}$ in scientific notation, magnetic moment in Bohr Magnetons. Fe[Cl_{16}Pc(-2)] Mol.wt. = 1119.4, diamagnetic correction = 617 x 10^{-6} $cm^3 mol^{-1}$: 5.41 1.059E-01, 2.140; 7.93 9.650E-02, 2.474; 12.65 7.771E-02, 2.804; 17.35 6.361E-02, 2.971; 22.11 5.307E-02, 3.063; 27.10 4.469E-02, 3.112; 32.21 3.825E-02, 3.139; 36.95 3.357E-02, 3.150; 41.65 2.986E-02, 3.154; 45.35 2.755E-02, 3.161; 49.51 2.502E-02, 3.148; 54.28 2.292E-02, 3.154; 59.26 2.104E-02, 3.158; 64.54 1.929E-02, 3.155; 70.08 1.784E-02, 3.162; 75.21 1.662E-02, 3.161; 80.17 1.557E-02, 3.160; 84.68 1.467E-02, 3.152; 92.91 1.336E-02, 3.151; 103.22 1.204E-02, 3.153; 113.95 1.093E-02, 3.156; 125.00 1.005E-02, 3.169; 135.20 9.319E-03, 3.174; 145.27 8.709E-03, 3.181; 164.53 7.743E-03, 3.192; 184.33 6.929E-03, 3.196; 204.69 6.299E-03, 3.211; 225.21 5.776E-03, 3.225; 246.68 5.348E-03, 3.248; 261.61 4.983E-03, 3.229; 281.29 4.681E-03, 3.245; 297.53 4.491E-03, 3.269.

Co[Cl_{16}Pc(-2)] Mol.wt = 1123, diamagnetic correction 617 x 10^{-6} $cm^3 mol^{-1}$:- 5.27 6.864E-03, 0.538; 7.57 5.423E-03, 0.573; 12.48 4.173E-03, 0.645; 17.18 3.687E-03, 0.712; 21.93 3.416E-03, 0.774; 26.95 3.236E-03, 0.835; 32.08 3.125E-03, 0.895; 36.81 3.050E-03, 0.948; 41.61 3.000E-03, 0.999; 45.23 2.980E-03, 1.038; 49.39 2.983E-03, 1.085; 54.10 3.010E-03, 1.141; 59.07 3.009E-03, 1.192; 64.34 2.939E-03, 1.234; 69.49 2.907E-03, 1.271; 74.52 2.871E-03, 1.308; 79.49 2.847E-03, 1.345; 84.10 2.825E-03, 1.378; 92.64 2.789E-03, 1.438; 103.38 2.745E-03, 1.506; 113.56

2.697E-03, 1.565; 124.59 2.649E-03, 1.625; 134.68 2.597E-03, 1.673; 144.68 2.550E-03, 1.718; 163.94 2.451E-03, 1.793; 183.62 2.344E-03, 1.855; 203.83 2.256E-03, 1.918; 224.47 2.172E-03, 1.974; 245.48 2.089E-03, 2.025; 264.22 2.019E-03, 2.065; 280.33 1.957E-03, 2.095; 296.47 1.917E-03, 2.132.

PTIR data: (Nujol Mulls) **1** ; 721m, 753m, 772s, 780sh, 956s, 1100m, 1158vs, 1214vs, 1274s, 1308vs, 1313m. **2**; 722w, 747s, 771s, 779m, 941vs, 1099m, 1142vs, 1207s, 1274m, 1302s, 1320m, 1326m. **3**; 722m, 752m, 772m, 780w, 957m, 1096s, 1160s, 1215vs, 1275s, 1305m, 1315m.

Solutions for spectroscopy, electrochemistry and spectroelectrochemistry were prepared in DMF (Aldrich, Gold Label). Solutions for spectroelectrochemistry, cyclic voltammetry and differential pulse polarography contained 0.1M LiCl (recrystallized from water and dried under vacuum) as supporting electrolyte and were maintained under nitrogen. Spectra were recorded in DMF which had been deoxygenated either by bubbling with nitrogen or by several freeze-pump-thaw cycles.

Buffer solutions were prepared from 0.1M solutions of reagent grade H_3PO_4, KH_2PO_4, K_2HPO_4 and KOH, and adjusted to the desired pH, and approximately constant ionic strength. Distilled water for buffer solutions was double distilled in glass from alkaline $KMnO_4$, then passed through a Barnstead organic removal cartridge and two Barnstead mixed resin ultrapure cartridges. Argon, nitrogen and oxygen were used as supplied. Buffer solutions were saturated with argon or oxygen for about 1 hour, and maintained under an atmosphere of the appropriate gas during data collection. Oxygenated solutions contained an oxygen concentration of approximately 10^{-3} M.

Electronic spectra were recorded with a Hitachi-Perkin Elmer Model 340 microprocessor-controlled spectrometer, or a Guided Wave Inc. Model 100-20 optical waveguide spectrum analyzer. Spectroelectrochemical data were recorded as for spectra, using a PAR Model 173 potentiostat with a two-compartment cell. A

platinum-junction SCE, separated from the working electrode with a Luggin capillary for contact, served as a reference. A platinum basket was employed as the working electrode, and the auxiliary electrode was a platinum wire separated from the bulk of the solution by a ceramic frit. Spectra were recorded during bulk electrolysis by immersing the fibre optic probe in the solution,[14] or by using a cell with inset windows for use with a conventional spectrometer.

Modified HOPG electrodes were prepared as previously described[15,16] and the catalyst was adsorbed for about 30 minutes (minimum time to ensure equilibrium adsorption) from solutions of 0.5 - 1 $x10^{-4}$M in DMF.

Results and Discussion

Electronic and Geometric Structure

i) Magnetism

The iron complex 1 is a typical iron(II) square planar phthalocyanine with no axial coordination. Its room temperature magnetic moment is 3.27BM compared with 3.85 BM for unsubstituted FePc,[17-19] and attributable to intermediate spin S=1.

The magnetic properties follow the Curie-Weiss law with an apparent Curie-Weiss constant of -4.9 K (see expt. section). However, as shown in Fig.1, there is a sharp reduction in magnetic moment occurring below about 25 K, falling to 2.14 BM at 5 K. This behaviour is remarkably similar to that of unsubstituted FePc except that in this latter case, the sharp reduction in magnetic moment begins at about 60 K.[18]

The magnetic properties of FePc are well described in terms of a $^3B_{2g}$ ground term with zero field splitting, D, of the M_s = 0 (lowest) and M_s = ± 1 magnetic spin components. The relevant parameters are $g_{II} = g_{\perp} = 2.74$ and D = 64 cm^{-1}.[18]

If exactly the same model is used to explain the magnetic data for species 1, then an adequate fit of the average magnetic moment can be obtained with the

parameters g_{II} = 2.22, $g_{\perp}$ = 2.28, D = 16 cm^{-1} and T.I.P. = 140 x 10^{-6} $cm^3 mol^{-1}$ (Fig. 1). A detailed single crystal anisotropy study is necessary to prove the validity of this data set since the fit is not unique. Within this model, the sharp decrease in magnetic moment near 20 K does require D to lie in the range 17 ± 5 cm^{-1}, while the fit at higher temperatures requires the average g value to be close to 2.26 ± .05; however the individual g values may deviate from the values quoted here. The lower moment, of 1 relative to FePc, can be explained in terms of changes in the coupling of ground to excited state terms (variation in g factor) rather than in an exchange coupling mechanism which does not need to be introduced.

The cobalt complex 3 exhibits a room temperature magnetic moment of 2.13 BM compared with 2.72BM for CoPc[17,20,21] and associated with an S = 1/2 intermediate spin square planar cobalt(II) phthalocyanine. However the temperature dependence is unusual. Down to about 50 K, the susceptibilty follows the Curie-Weiss Law but with an apparent Curie-Weiss constant of -350 K, (Fig.1). Below 50 K the susceptibility increases rapidly indicating a change in the coupling process has occurred.

Unsubstituted CoPc shows only a relatively small change in magnetic moment between room temperature and 80 K and fits a simple model involving a d_{z^2} ground state.[20,21] This model is quite unable to explain the behaviour of the cobalt species, 3. It is likely that there is an exchange process occurring in this system but single crystal anisotropy studies are needed to unravel this distinctive behaviour.

ii) Solubility

These three complexes have exceedingly low solubilities in essentially all solvents which leads to considerable difficulty in obtaining reliable data therefrom. Sonication in solvents such as DMF or DMSO leads to a moderately strongly coloured solution, but such "solutions" generally dropped some sediment upon standing - it is likely that they are not true solutions. The addition of electrolyte (e.g., tetrabutylammonium hexafluorophosphate ($TBAPF_6$) and

tetrabutylammonium perchlorate (TBAP)) to DMF "solutions" prompted the complexes to precipitate, causing difficulty in obtaining solution electrochemical data of high quality. Indeed on standing overnight, such solutions become colorless.

The addition of chloride ion, does lead to slightly greater solubility, via complexation, especially for the oxidized species. The addition of hydrazine causes greater solubility of the iron and zinc complexes, also because of complexation, but causes reduction of the cobalt complex.

Because of these problems spectroelectrochemical studies, with one exception, did not yield isosbestic points as is commonly expected in such experiments,[22,23], and molar extinction coefficients are not reliably obtained.

Nevertheless, it is possible to obtain definitive characterisation data for these species in order to investigate the effect of 16 chlorine substituents upon their chemistry.

iii) Electronic Spectra

a) **Organic solvent data:-** Complexes 1, 2, and 3 when freshly "dissolved" in nitrogen-purged DMF, yield the electronic spectra shown in Fig.2. The cobalt and zinc species spectra are typical of aggregated phthalocyanine with dilution having little effect upon the spectrum. The iron complex, 1, spectrum, is that of a largely non-aggregated iron(II) phthalocyanine.[15,24] The presence of the charge transfer band in the region 400 - 500nm is typical of an axially-coordinated iron(II) phthalocyanine.[24-27] There is some variability in these spectra from one sample to the next.

If 1 is "dissolved" in aerated DMF, or the nitrogen purged solution is allowed to absorb oxygen, or faster if the solution is heated in the presence of oxygen, the Q band broadens and shifts to the blue (Table 1). Upon reduction of this oxidized solution, the higher energy component of the Q band diminishes first in intensity relative to the lower energy component; there is no similar change in

intensity when the species is oxidized. It is most likely that 1 forms a μ-oxo dimeric species, $\underline{[Cl_{16}Pc(-2)]Fe(III)\text{-}O\text{-}Fe(III)[Pc(-2)Cl_{16}]}$ (4) when "dissolved" in aerated DMF - such species typically absorb strongly near 620 nm.[28-31] This species, 4, reverts to 1 when heated in degassed DMF. It was not isolated.

The redox species accessible to these various complexes were determined by spectroelectrochemical studies. When reduced in DMF/LiCl at -0.80V vs SCE, species 1 yields a spectrum typical of $[Fe(I)Pc]^-$ (Table 1).[32,33] Re-oxidation at 0.00V regenerates the Fe(II)Pc spectrum (Table 1). Solubility problems and the absence of isosbestic points prevent an analysis using the Nernst equation to determine the precise position of the Fe(II)/Fe(I) couple. However the $Fe(II)[Cl_{16}Pc(-2)]/Fe(I)[Cl_{16}Pc(-2)]^-$, couple must lie between 0.00 and -0.80V vs SCE under these conditions.

When oxidized at 0.65V vs SCE, the characteristic Fe(II)Pc charge transfer band observed near 500 nm for species 1 in DMF/LiCl diminished in intensity relative to the Q band but a completely oxidized Fe(III)Pc species was not obtainable below the solvent oxidation limit. Thus the $Fe(III)[Cl_{16}Pc(-2)]^+/Fe(II)[Cl_{16}Pc(-2)]$ solution oxidation potential for species 1 is near and possibly slightly above 0.65V in DMF/LiCl.

Reduction of the zinc species, 2, in DMF/LiCl, did yield isosbestic points (Fig.3) showing reduction to $\underline{Zn(II)[Cl_{16}Pc(-3)]^-}$ (5) in a clean process where the reduced species could be re-oxidized to starting species 2. An analysis using the Nernst equation yielded a redox potential of -0.60V vs SCE for the $Zn(II)[Cl_{16}Pc(-2)]/Zn(II)[Cl_{16}Pc(-3)]^-$ redox process. Fig.3 also shows data for further reduction to the presumed $\underline{Zn(II)[Cl_{16}Pc(-4)]^{2-}}$ species, (6). The isosbestic points are lost in this second reduction, but re-oxidation does regenerate species 2.

The spectrum of complex 3 (Fig. 2) is dominated by aggregation, indicated by the very broad Q-band[27,35,36] with a blue-shifted component near 640nm.

Addition of hydrazine, or NaSH, to a DMF solution of complex 3, yields a spectrum typical of a Co(I)Pc species (Table 1).[24,25,33,36] The same species is obtained by electrochemical reduction of a solution of 3 in DMF/LiCl at -0.8V vs SCE. Re-oxidation at 0.0V yields a spectrum with a double Q band similar to that initially observed (Fig.2). The Co(II)[Cl_{16}Pc(-2)]/Co(I)[Cl_{16}Pc(-2)]$^-$ couple must lie between 0.00 and -0.80V vs SCE in DMF/LiCl.

Oxidation of 3 in DMF/LiCl, at 0.9V yields a spectrum in which the Q band, centered at 690nm, is relatively stronger and sharper; most of the higher energy Q component, observed in the spectrum of the cobalt(II) species, disappears, but there is no growth of absorption near 450-550nm. This behaviour is typical of the formation of a Co(III)[Cl_{16}Pc(-2)]$^+$ species which, however, could not be produced fully before the solvent oxidation limit.

Table 1 shows the data for these species in various oxidation states and data from the literature for unsubstituted or tetraneopentoxy substituted phthalocyanines. In general there is close agreement between the relevant sets of data providing further support for the oxidation state conclusions reached here. An apparent exception is the Zn(II)[Cl_{16}Pc(-3)]$^-$ (5) anion radical whose electronic spectrum appears rather different from that previously described for the unsubstituted Zn(II)Pc(-3) anion radical (7).[33] However closer examination shows significant similarity. Species 7 shows three absorption features between 25,000 and 15,000 cm^{-1}, one being a well defined shoulder on the Soret region absorption. A fourth transition is evident as an ill-defined shoulder on the upper energy Q band component.[37] In the spectrum of anion radical 5, the shoulder on the Soret is red-shifted and now appears as a well defined, narrow, peak, while the upper energy component of the Q band absorption is now clearly two absorptions.

There is a general trend that, with few exceptions, any given band (Q band, Soret or charge transfer) in the spectrum of a M[Cl_{16}Pc(-2)] species is shifted slightly to lower energy relative to the corresponding transition in the spectra of

the other derivatives cited.

b) **Concentrated sulphuric acid data:-** The three complexes dissolve in concentrated sulfuric acid without decomposition; their spectra are listed in Table 2, along with the corresponding data for various other substituted and unsubstituted MPc derivatives. The striking aspect of the data is the very significant red shift in the position of the Q-band. The position of the Q-band in the sulfuric acid spectrum should be a measure of the basicity of the uncoordinated bridging nitrogen atoms in the macrocycle.[38,39] It is influenced critically by the nature and position of the phthalocyanine peripheral substituents.

Comparing the data in Table 2, however, there is no simple relationship between substituent donicity and Q-band wavelength maximum. For example, within the group of copper phthalocyanines, electron donor substituents are seen to shift the maxima both to higher and lower wavelength relative to the unsubstituted species. In general, halogen substituents shift the Q band maximum to longer wavelengths relative to the unsubstituted species, with chloride substitution being more effective than fluoride substitution in this respect. The observed shift probably involves a subtle interplay of the inductive and mesomeric properties of the substituent, and its location on the peripheral benzene ring.

Using Forster theory[40,41] a red shift in the Q band absorption would signify that the excited state was a stronger base than the ground state. Thus perchlorination has a substantial effect in increasing the basicity of the excited state relative to the ground state. Chloride substitution is expected to stabilise both the π and π^* states of the phthalocyanine ring.[42] The HOMO a_{2u} orbital has nodes at the peripheral nitrogen atoms, while the LUMO e_g orbital does have electron density at these positions.[42] Thus protonation of any phthalocyanine will red shift the π-π^* transition relative to the unprotonated species, as is indeed evident.[43] To understand the reasons for the extraordinary red shifts seen with these species requires further experiment.

iv) Fourier Transform Infrared Spectroscopy

All three species have very similar FTIR spectra (see expt. section) suggesting a similar crystal structure, though the data for iron and cobalt are more closely similar than for zinc.

v) Electrochemistry

Electrochemical studies of 1, 2, and 3 were carried out both with the complexes in solution and as a modifier on a Highly Oriented Pyrolytic Graphite (HOPG) electrode.

The surface electrochemistry was generally reproducible, though the first scan of a M[Cl_{16}Pc(-2)]-modified electrode was somewhat different from all subsequent scans. If the complexes are being deposited in an aggregated form, the adsorbed molecules may rearrange on the surface during the initial scanning process. Moreover many of the redox waves seen in the study of these species were structured with shoulders suggesting that there were several slightly different sites on the HOPG surface. All the waves have their current linearly dependent on scan rate indicative of a surface rather than diffusion process.

The zinc species is the easiest to understand and its analysis provides useful data for interpreting the iron and cobalt data. Thus Fig.4 shows data for zinc species 2 deposited on HOPG at low and high pH. In the range studied, one observes only one redox couple whose $E_{1/2}$ (average of anodic and cathodic peak) potential depends upon pH (Table 3). The anodic and cathodic peak potentials are within 100mV of each other at all pH values studied, but with the greatest disparity occuring in strong base (Table 3). In this sense the couple is reasonably reversible. The anodic and cathodic peak components do depend slightly on scan rate with their separation increasing with increasing scan rate (as is also observed in the iron and cobalt species voltammograms). This couple can only be assigned to the ring

$Zn[Cl_{16}Pc(-2)]/Zn[Cl_{16}Pc(-3)]^-$ reduction process. The charge under the reduction peak is about 4 micro Coulombs. Assuming the graphite surface is flat, and that the phthalocyanine molecules occupy an area of about 2×10^{-14} cm^2, this corresponds to a monolayer of dimeric aggregates.

In Table 4 we compare the potentials for a range of phthalocyanine species both in solution and adsorbed on a graphite surface. Two general observations may be made;

a) The ring Pc(-2)/Pc(-3) reduction process occurs at similar potentials in DCB solution and on an HOPG surface, when this is immersed in aqueous base solution.

b) Electron acceptor substituents will shift the reduction couple to more positive potentials, while electron donor substituents will shift it to more negative potentials. For example note the DMF solution data for zinc phthalocyanines in Table 4 where octacyano substitution shifts this potential 760mV positive of the unsubstituted ZnPc potential, while octabutoxy substitution shifts it 200 mV more negative.

Following items (a,b), using the datum for $Zn[Cl_{16}Pc(-2)]$/HOPG immersed in aqueous base at pH 10-13 the reduction process shifts positively in the sequence TNPc = OBuPc < Pc < $[Cl_{16}Pc(-2)]$ << OCNPc. Thus perchlorination makes the phthalocyanine ring a better acceptor but not to a dramatic degree.

The iron species 1, adsorbed on HOPG, shows a well behaved couple positive of zero whose identity, based upon previous iron studies[44] is ascribed to $Fe(III)[Cl_{16}Pc(-2)]^+/Fe(II)[Cl_{16}Pc(-2)]$ (Fig.5). The anodic and cathodic peak potentials do not differ significantly from each other throughout the pH range (Table 3). At any given pH its potential is more positive than for FePc or FeTsPc (Table 4) also indicative of the acceptor nature of the chlorine substituents. The corresponding $Co(III)[Cl_{16}Pc(-2)]^+/Co(II)[Cl_{16}Pc(-2)]$ couple is expected at very positive potentials in the voltammogram of species 3, based upon previous experience,[44] and was not observed in the surface electrochemistry.

Both iron 1 (Fig.5) and cobalt 3 species (Figs.6,7) show a well defined reduction wave whose potential is pH dependent throughout the pH range studied (1-14), (Fig.8) (Table 3). Both species show additional weak, poorly resolved, waves on the positive side of the reduction wave, (vide infra).

The strong reduction wave can be ascribed to one of three plausible processes, $M(II)[Cl_{16}Pc(-2)]/M(I)[Cl_{16}Pc(-2)]^-$, $M(II)[Cl_{16}Pc(-2)]/M(II)[Cl_{16}Pc(-3)]^-$ and $M(I)[Cl_{16}Pc(-2)]^-/M(I)[Cl_{16}Pc(-3)]^{2-}$ where this last possibility must assume that the $M(II)[Cl_{16}Pc(-2)]/M(I)[Cl_{16}Pc(-2)]^-$ is accounted for by the weaker poorly resolved structure positive of the main reduction wave.

Spectroelectrochemistry in solution (above) shows that reduction to $M(I)[Cl_{16}Pc(-2)]^-$ occurs above -0.8V in DMF but this datum does not necessarily provide rigorous information for the adsorbed species.

In determining the nature of this reduction wave, certain observations can be made:-

c) Previous pH dependence studies of the $M(II)Pc(-2)/[M(I)Pc(-2)]^-$ process show that the potential is dependent upon pH in the acidic range, but independent of pH in the basic range.[44-48]

d) Previous pH dependence studies of the $[M(I)Pc(-2)]^-/[M(I)Pc(-3)]^{2-}$ process show that the potential is dependent upon pH through the entire pH range.[44]

e) Previous studies of the $[M(I)Pc(-2)]^-/[M(I)Pc(-3)]^{2-}$ redox couple reveal that it is often much stronger and narrower than the $M(II)Pc(-2)/[M(I)Pc(-2)]^-$ redox process, especially in the alkaline regime.[44]

f) The $M(II)Pc(-2)/[M(II)Pc(-3)]^-$ process has never been observed for MPc = CoPc or FePc. On the basis of the polarising power of the central ion[49] this couple would be expected to occur slightly positive of the corresponding zinc couple.

g) The $M(II)Pc(-2)/[M(I)Pc(-2)]^-$ and $[M(I)Pc(-2)]^-/[M(I)Pc(-3)]^{2-}$ redox couples are within about 100-300 mV of each other in the acidic range but their separation increases as pH increases above 7 because of their different pH dependence in this

range.[44]

h) The Zn(II)Pc(-2)/[Zn(II)Pc(-3)]$^-$ process occurs some 300-500 mV more positive than the [M(I)Pc(-2)]$^-$/[M(I)Pc(-3)]$^{2-}$ process (M = Co,Fe) in solution, depending upon substituent.[22,23] However this difference is somewhat smaller when the species are in the adsorbed state.

i) At any pH value, the first reduction wave of Zn[Cl_{16}Pc(-2)], 2, occurs at a less negative potential than the primary reduction wave of either iron 1 or cobalt 3.

j) Perchlorinated phthalocyanine is a better acceptor ligand than Pc or TNPc. Not only will the M(III)[Cl_{16}Pc(-2)]$^+$/M(II)[Cl_{16}Pc(-2)] (M=Co,Fe) wave be at a more positive potential than for MPc, MTsPc or MTNPc, but the M(II)[Cl_{16}Pc(-2)]/M(I)[Cl_{16}Pc(-2)]$^-$ and M(I)[Cl_{16}Pc(-2)]$^-$/M(I)[Cl_{16}Pc(-3)]$^{2-}$ waves should also lie at more positive potentials, for corresponding M.

Items (c)-(j) lead to only one tenable assignment for the reduction couple.

Thus: assignment to the M(II)[Cl_{16}Pc(-2)]/M(II)[Cl_{16}Pc(-3)]$^-$ process is excluded because observation (f) is incompatible with observation (i). Assignment to the M(II)[Cl_{16}Pc(-2)]/M(I)[Cl_{16}Pc(-2)]$^-$ process is excluded because it could not be found so negative of the zinc couple in the basic range. If, energetically, such a process was very negative of the zinc couple, then reduction to M(II)[Cl_{16}Pc(-3)]$^-$ would have to occur first, and this has already been excluded. Moreover the pH dependence is not appropriate for this assignment.

However assignment to the M(I)[Cl_{16}Pc(-2)]$^-$/M(I)[Cl_{16}Pc(-3)]$^{2-}$ process does not violate any of the observations noted above. Indeed such an assignment is specifically supported by the observed pH dependence, by the very narrow intense peak for this redox process, by the fact that it is observed negative of the corresponding zinc process at all pH values, and because it occurs several hundred millivolts positive of the corresponding waves in the MPc and MTsPc species, at any given pH.

Both the iron and cobalt species, but not the zinc species, show a poorly

resolved shoulder around 100mV positive of the reduction wave in the acidic range. This is assigned to the M(II)[Cl_{16}Pc(-2)]/[M(I)[Cl_{16}Pc(-2)]$^-$ wave. In alkaline medium many of these species also show a more pronounced wave, positive of the reduction wave and close to or identical with the potential at which oxygen reduction occurs at the relevant pH value (Table 3) (Fig.8). This might arise from the M(II)[Cl_{16}Pc(-2)]/[M(I)[Cl_{16}Pc(-2)]$^-$ process but it may also be due to residual oxygen trapped in the electrode or leaking back slowly into the electrolyte despite the argon flow. This is demonstrated in Fig.9 where a small amount of oxygen has deliberately been admitted into the system, to delineate clearly the oxygen reduction potential in the presence of only trace oxygen.

Differential pulse voltammetry has been carried out on the cobalt species 3 adsorbed on HOPG. A typical example is shown in Fig.7 where the modified HOPG electrode is immersed in buffer at pH 4. The broad cyclic voltammetric wave is clearly split into two components in the differential pulse voltammogram. These may be the first two reduction processes, to Co(I)[Cl_{16}Pc(-2)]$^-$ and then Co(I)[Cl_{16}Pc(-3)]$^{2-}$ but may also represent two different sites on the surface for the same reduction process.

Thus the main reduction wave seen in all three complexes is the ligand - anion radical wave of zinc(II), cobalt(I) and iron(I).

pH Dependence: Reduction couple: All three species show a similar pH dependence; the iron species 1 was chosen for the most detailed analysis. Thus the anodic and cathodic peak components shift to more negative potentials with increasing pH, throughout the entire pH range studied (1-14). The actual positions of the reduction peaks and their degree of structure are somewhat sensitive to variation in surface morphology from one surface to another. The separation between the peak potentials also tends to increase with increasing pH (see Table 3, Fig.8). However the average peak positions are reproducible (error ± 20mV). The best lines are:-

(data in volts for $M[Cl_{16}Pc(-2)]/M[Cl_{16}Pc(-3)]^-$).

Iron (1) E = -0.064pH - 0.11 R = 0.997 for 23 points

Zinc (2) E = -0.060pH - 0.06 R = 0.998 for 7 points

Cobalt (3) E = -0.069pH - 0.20 R = 0.999 for 9 points

The most reasonable explanation of the pH dependence follows from the fact that the potential in organic solvents is most similar to that in basic media. Under such circumstances the molecule being reduced in solution is essentially the same as that on the surface. However with decreasing pH, protonation occurs at the peripheral nitrogen atoms because the phthalocyanine is negatively charged for zinc and di-negatively charged for iron and cobalt.

The increasing separation between anodic and cathodic peak components at higher pH is much more pronounced for iron and cobalt than for zinc. Once the material is reduced there is evidently some change in electronic structure such that the reduced material becomes more difficult to oxidize. Since this occurs to a greater degree with the dinegative species than with the mononegative reduced 2, it may be a consequence of enhanced binding to the graphite surface by the iron and cobalt species in their dinegative reduced state.

The $Fe(III)[Cl_{16}Pc(-2)]^+/Fe(II)[Cl_{16}Pc(-2)]$ couple is dependent upon pH across the entire pH range studied (1-14). The equation of the line is, for species 1:- (Data in volts).

$E(Fe^{III}/Fe^{II})$ = -0.056pH + 0.72 R = 0.990 for 18 points.

This is a surprising result clearly induced by the perchlorination substitution. Previous studies of the Fe(III)/Fe(II) redox process in iron phthalocyanine species have shown that this couple is independent of pH in the acidic region, but has an

approximately -59mV/pH dependence in the basic regime.[44]

The pH dependence in the alkaline regime is readily explained in terms of the binding of an OH^- group to $\underline{Fe(III)[Cl_{16}Pc(-2)]^+}$, and its absence from $\underline{Fe(II)[Cl_{16}Pc(-2)]}$ or perhaps more likely, two OH^- bound to Fe(III) and one bound to Fe(II).

In the acidic range one might consider protonation of peripheral nitrogen atoms. However since this pH dependence is not observed in the unsubstituted FePc case, and since chlorination should reduce the basicity of these nitrogen atoms, such an explanation is not viable. Rather a water molecule may bind to $\underline{Fe(III)[Cl_{16}Pc(-2)]^+}$ and is rendered rather acidic by the acceptor nature of the chlorine substitution.

Solution Electrochemistry (Table 5)

Very dilute, apparently true solutions of $\underline{Zn[Cl_{16}Pc(-2)]}$ (2) in DMF/TBA PF_6 show two reversible reduction waves separated by some 300mV and evidently only to be associated with the two expected $Zn(II)[Cl_{16}Pc(-2)]/Zn(II)[Cl_{16}Pc(-3)]^-$ and $Zn(II)[Cl_{16}Pc(-3)]^-/Zn(II)[Cl_{16}Pc(-4)]^{2-}$ anion radical reduction processes.[22,50] The potential is similar to that of the surface under mild basic conditions (see (a) above). The voltammetry is consistent with the Nernst analysis of the data shown in Fig.3 and described above (but note different solvent system).

Oxidation waves near 0.6 and 1.0 V (vs SCE) observed for the iron 1 and cobalt 3 species when "dissolved" in DMF/TBAPF$_6$ are readily associated with the $M(III)[Cl_{16}Pc(-2)]^+/M(II)[Cl_{16}Pc(-2)]$ redox process (M = Fe,Co). Scanning negatively therefrom, the first reduction waves are seen near -1.2 - -1.3V for both species. These waves cannot be associated with the $M(II)[Cl_{16}Pc(-2)]/[M(I)[Cl_{16}Pc(-2)]^-$ redox process since they are found significantly negative of those $M(II)Pc(-2)/[M(I)Pc(-2)]^-$ processes unequivocally identified in the voltammograms

of CoTNPc and MTsPc (M=Co,Fe) (Table 4) (Data for FeTNPc are not available). On the basis of the acceptor character of the chlorine substituents, such a process should be found positive of that observed in these latter species. The observed reduction waves are also considerably negative of the -0.8V which the spectroelectrochemical studies showed to be more negative than the $M(II)[Cl_{16}Pc(-2)]/[M(I)[Cl_{16}Pc(-2)]^-$ couple.

However, these waves do occur at a similar position to the $M(I)[Cl_{16}Pc(-2)]^-, M(I)[Cl_{16}Pc(-3)]^{2-}$ surface wave when the modified electrode is immersed in strong alkaline medium. Thus these solution reduction waves are assigned to $M(I)[Cl_{16}Pc(-2)]^-/M(I)[Cl_{16}Pc(-3)]^{2-}$, M = Co,Fe. Evidently in parallel with the surface electrochemistry, the $M(II)[Cl_{16}Pc(-2)]/[M(I)[Cl_{16}Pc(-2)]^-$ couples for these perchlorinated phthalocyanines are broadened too much for observation, likely a consequence of aggregation and an associated slow kinetic pathway for electron transfer to the aggregate.

In a similar fashion to the zinc species 2, both the cobalt and iron species show a second reduction process some 0.4 - 0.6V more negative than the first. This may then be assigned to the $M(I)[Cl_{16}Pc(-3)]^{2-}/M(I)Cl_{16}Pc(-4)]^{3-}$ redox process, by analogy with previous solution observations.[22,50]

In conclusion the solution data do support the assignments made for the surface electrochemistry.

Electrocatalytic Oxygen Reduction

HOPG surfaces modified with 1 or 3 reduce oxygen electrocatalytically in a manner parallel to that observed with MPc,[50-55] CoTNPc,[15,16] and MTsPc (M=Co, Fe) species.[44,56,57] As shown in Fig. 8, for species 1, the peak potential for oxygen reduction is a function of pH only in acidic solutions where the slope of $E_p(O_2)$ vs. pH is -(65-75) mV per pH unit. The cobalt species 3 reduces oxygen in the usual

two-electron reduction to hydrogen peroxide, and is also pH independent in the alkaline range (Table 3). This conclusion arises from ring-disk experiments (not described in detail here) which show, at pH 10.1, hydrogen peroxide at the ring, formed concomitantly with oxygen reduction at the disk, when cobalt species 3 is the electrocatalyst.

The number of electrons involved in the iron 1 catalysed reduction of oxygen is less certain due to poor reproducibility of current from one experiment to another (different surfaces). In alkaline medium, FePc is expected to be a four-electron reductant of oxygen to molecular oxygen (Fig.9). When iron species 1 is the electrocatalyst, at pH 10.1, in a ring-disk experiment, oxygen reduction occurring in the range 0 - -0.35V (the peak of the cyclic voltammogram for oxygen reduction) (Fig.9) apparently produces water, there being no appreciable ring current. At potentials more negative than -0.35V, oxygen reduction is associated with hydrogen peroxide detection at the ring. It seems secure that, like FePc, Fe[Cl_{16}Pc(-2)] also acts as a four electron catalyst in what is evidently a complex multi-path oxygen reduction process.[45]

The low solubility of both the iron and cobalt species leads to some scatter in the oxygen reduction data. Since oxygen reduction at phthalocyanine modified electrodes has been very extensively studied previously[15,16,44,50-58] further discussion is not warranted here.

Note, Fig.9, that oxygen reduction occurs some 800mV more positive than the principal reduction wave at pH 14. Previous studies[15] reveal that oxygen reduction generally occurs close to or slightly positive of the M(II)Pc(-2)/[M(I)Pc(-2)]$^-$ couple and thus this observation provides further evidence that the principal reduction wave near -1.1 volts, (in Fig.9) cannot be the M(II)[Cl_{16}Pc(-2)]/[M(I)[Cl_{16}Pc(-2)]$^-$ reduction process.

Oxygen reduction, using 3, occurs at a potential some 150-250mV more positive than was observed with CoTNPc,[15] consistent with the stronger acceptor nature of

the catalyst molecule. Previous studies have shown that the oxygen reduction potential tracks the pH dependence of the Co(II)/Co(I) couple.[15] Since this oxygen reduction potential, in the acidic range, is about 100 mV positive of the main reduction wave, now assigned to $M(I)[Cl_{16}Pc(-2)]^-/M(I)[Cl_{16}Pc(-3)]^{2-}$, the inference is that the $M(II)[Cl_{16}Pc(-2)]/[M(I)[Cl_{16}Pc(-2)]^-$ couple is very close to and perhaps partially obscured by the main reduction process. This adds support to the argument that the $M(II)[Cl_{16}Pc(-2)]/[M(I)[Cl_{16}Pc(-2)]^-$ process is represented by the shoulder on the positive potential side of the main reduction wave in acidic medium.

Conclusions

Perchlorination of the phthalocyanine ring leads to derivatives whose properties are clearly modified by the electron withdrawing substituents. The species are much easier to reduce but more difficult to oxidize. The change in pH dependence for the $Fe(III)[Cl_{16}Pc(-2)]^+/Fe(II)[Cl_{16}Pc(-2)]$ couple relative to unsubstituted FePc reveals a new procedure for the tuning of a redox potential, in this case through a combination of pH control and ring substitution. In particular the central metal ion has gained additional Lewis acid character. The lack of clear observation of the $M(II)[Cl_{16}Pc(-2)]/M(I)[Cl_{16}Pc(-2)]^-$ redox process may arise through very sluggish kinetics, a consequence of the chlorine substitution generating aggregates, and causing the wave to be broadened over an appreciable potential range. Further studies with other central metal ions are likely to prove rewarding.

Acknowledgements: The authors are indebted to the Natural Sciences and Research Council (Ottawa) and to the Office of Naval Research (Washington) for financial support.

No Fee

Figure Legends

Fig.1 Magnetic data for upper) iron (1) and lower) cobalt (3) species. The open triangles show the magnetic moment data using the right-hand y axis, while the open circles illustrate the magnetic susceptibility and use the left-hand axis. The solid lines through the iron data are those calculated on the basis of model of the $^3B_{2g}$ ground term split by the zero field. See text for details and parameters.

Fig.2 Electronic spectroscopic data for species 1, 2 and 3 "dissolved" in argon purged DMF.

Fig.3 Spectroelectrochemical data for the reduction of zinc species 2, in DMF containing 0.1M LiCl. The successive spectra are obtained with the platinum working electrode polarised at 0.0V (a), -0.6 (b), -0.7 (c) -0.8 (d) and -1.3V (e). Spectrum (a) corresponds with the starting material 2, spectrum (d) is dominantly that of the anion radical 5 with a small contribution from that of the di-anion radical 6. Spectrum (e) is that of the di-anion radical 6.

Fig.4 Surface electrochemical cyclic voltammograms for zinc species 2 under Argon at lower) pH = 12.5, middle) pH = 6 and upper) pH = 4. Scan rates are 150, 80 and 100 mV/s respectively but each surface is a new surface and therefore the quantity of material varies from one plot to the next. Each division on the y axis corresponds to 10 microamps.

The horizontal lines through each voltammogram are the zero current axes for the respective voltammogram. All scans here and in later Figures were initiated from positive towards negative potentials and are shown with the cathodic (reduction) current at the bottom. They are all equilibrium scans.

Fig.5 Surface electrochemical cyclic voltammograms for iron species 1 under argon at lower) pH = 11, middle) pH = 5.7, and upper) pH = 2. Scan rates 100, 200 and 100 mV/s respectively. The y axis divisions are 10 microamps. For other

notes see Fig. 4. Also see Fig.9 for further iron data.

Fig.6 Surface electrochemical cyclic voltammograms for cobalt species 3 under argon at lower) pH = 10, and upper) pH = 2. Scan rate 100mV/s and y axis scale divisions of 10 microamps. For other notes see Fig.4.

Fig.7 Surface electrochemical cyclic voltammogram for cobalt species 3 under Argon at pH = 4, scan rate 100 mV/s, The y axis divisions are 5 microamps. Superimposed is the surface electrochemical differential pulse voltammogram for cobalt species 3 at a scan rate of 1mV/s and pulse amplitude of 5mV. The y axis divisions are each 1 microamp for this plot. The plot is inverted from the more normal presentation to show reduction downwards.

Fig.8 The pH dependences of the various surface waves using a modified iron species 1 HOPG electrode immersed in an appropriate phosphate buffer. $Fe(III)[Cl_{16}Pc(-2)]^{+}/Fe(II)[Cl_{16}Pc(-2)]$ couple - open squares; $Fe(II)[Cl_{16}Pc(-2)]/Fe(I)[Cl_{16}Pc(-2)]^{-}$ couple - closed triangles; $Fe(I)[Cl_{16}Pc(-2)]^{-}/Fe(I[Cl_{16}Pc(-3)]^{2-}$ couple the open circles show the average potentials with the vertical bars indicating the anodic and cathodic component potentials. Their absence from a point means that the anodic-cathodic peak separation is less than 100mV. The oxygen reduction potentials are indicated by open triangles. NOTE: The bars shown here are NOT error bars.

Fig.9 Surface electrochemical cyclic voltammograms for iron species 1 on an HOPG surface. (Upper) under argon at pH = 14 (0.1M KOH) Scan rate 100mV/s, y axis scale divisions are 5 microamps apart.

(Lower) under an argon/oxygen mixture at pH = 14 (0.1M KOH). Scan rate 100mV/s, y axis scale divisions are 50 microamps apart. Only a dilute solution of oxygen in aq. KOH was added to demonstrate probable origin of the first negative reduction wave under argon.

Table 1 Electronic Spectra[a] (λ_{max} nm)

Complex	Note	Electronic spectra (nm)	Ref.
Fe(II)[Cl_{16}Pc(-2)]	(b)	361s 460 619 678s	tw
	(c)	345 641s 682sh	tw
	(d,e)	352 382 469 623 685s	tw
Fe(II)Pc(-2)	Py	324s 410m 654s	[15]
Fe(I)[Cl_{16}Pc(-2)]$^-$	DMF/LiCl	400br 537s 654w 687m 805m	tw
[(Py)Fe(I)Pc(-2)]$^-$	Py/LiCl	324s 512vs 596m 661m 803m	[32]
[Fe(I)Pc(-2)]$^-$	THF	326vs 515vs 596w 665m 800m	[33]
Co(II)[Cl_{16}Pc(-2)]	(b)	316s 360sh 490sh 641s 706sh	tw
Co(II)TNPc(-2)	DCB	330s 380m 612m 645sh 678vs	[23]
Co(I)[Cl_{16}Pc(-2)]$^-$	(d)	326s 480vs 545sh 656s 701s	tw
[Co(I)Pc(-2)]$^-$	THF	312vs 467s 633m 694s	[33]
[Co(I)TNPc(-2)]$^-$	DCB	313vs 471s 520sh 600sh 643m 675sh 708s	[23]
Zn[Cl_{16}Pc(-2)]	(b)	378s 404sh 660s 711s	tw
	(d,e)	362 404 649 688	tw
ZnTNPc(-2)	DCB	356vs 614m 680vvs	[22]
Zn[Cl_{16}Pc(-3)]$^-$	DMF/LiCl	415m 474m 600m 625sh 698m 830sh	tw
		860sh 894m 928m	tw
[ZnPc(-3)]$^-$	THF	323s 562s 636s 948m	[33]
Zn[Cl_{16}Pc(-4)]$^{2-}$	DMF/LiCl	363br 553s 696mbr 842m	tw

a) Absorption bands, for a specific metal and oxidation state and believed to have a common assignment, are lined up together in this Table. b) Argon purged DMF; c)

Aerated DMF - this is likely a solution of [Cl_{16}Pc(-2)]Fe(III)-O-Fe(III)[Cl_{16}Pc(-2)]; d) Argon purged DMF plus hydrazine. e) These species likely contain axially coordinated hydrazine;

Table 2 Spectroscopic Data for MX_nPc in Concentrated Sulfuric Acid; Position of the Q-Band

M	X[a]	n[b]	Q-Band Max.(nm)[c]	Ref.
CoPc	Cl	16	832	tw
CoPc	4-O-i-Pr	4	815	tw
CoPc	H	16	786	tw
CoPc	$4-CO_2H$	4	756	tw
CoPc	$3-NH_3$	4	738	[59]
CoPc	$3-NO_2$	4	715	
ZnPc	Cl	16	868	tw,[1]
ZnPc	4-O-NP	4	829	tw
ZnPc	4-OBu	4	827	[38]
ZnPc	F	16	820	[1]
ZnPc	H	16	783	[38]
ZnPc	CN	8	756	[38]
ZnPc	$4-NH_2$	4	742	[59]
FePc	Cl	16	854	tw
FePc	H	16	785	tw
FePc	$4-SO_3H$	4	770	tw
CuPc	F	16	821	[1]
CuPc	4-t-Bu	4	808	[43]
CuPc	4-Cl	4	803	[43]
CuPc	H	16	791	[43]
CuPc	4-Me	4	786	[43]
CuPc	$4-CO_2H$	4	780	[43]
CuPc	$4-NO_2$	4	776	[43]

CuPc	4-SO_3H	4	771	[43]
CuPc	CN	8	728	[39]
CuPc	3-NO_2	4	728	[43]
CuPc	3-CO_2H	4	722	[43]
CuPc	4-PhO	4	838	[39]
CuPc	4-NH_2	4	749	[59]
VOPc	4-Butyl	4	834	[60]
VOPc	Cl	16	862	[60]

a) Substituent. b) Number of substituents. b) Maximum wavelength component.

Table 3 Collection of Surface Electrochemical Data versus pH

$M[Cl_{16}Pc(-2)]/[MCl_{16}Pc(-3)]^-$

pH	Pc^a	Pa^b	$E_{1/2}^c$	$Fe^{II/Id}$	O_2 red^e	$Fe^{III/IIf}$
Iron data 1						
1.9	-0.23	-0.20	-0.22	-0.10(0.01)		0.63(0.08)
2.0	-0.24	-0.22	-0.23	-0.10(0.12)	-0.14	0.60(0.05)
2.6	-0.30	-0.24	-0.27			0.58(0.08)
2.6	-0.30	-0.24	-0.27			0.58(0.08)*g
3.0	-0.33	-0.29	-0.31		-0.265	
3.1	-0.36	-0.30	-0.33	-0.14(0.12)		0.52(0.06)
3.7	-0.40	-0.25	-0.32			0.53(0.06)*
3.8	-0.39	-0.31	-0.35	-0.19(0.13)		0.50(0.07)
4.0	-0.43	-0.33	-0.38		-0.29	0.47
4.7	-0.53	-0.32	-0.42			0.43(0.06)
5.0	-0.53	-0.37	-0.45		-0.34	
5.6	-0.56	-0.36	-0.46			0.42(0.075)*
5.7	-0.64	-0.34	-0.49			0.40(0.04)
6.0	-0.60	-0.36	-0.48		-0.30	
7.0	-0.65	-0.42	-0.53	-0.14	-0.27	0.34(0.08)*
8.0	-0.77	-0.48	-0.62		-0.26	
8.6	-0.82	-0.44	-0.63			0.27(0.04)*
8.8	-0.86	-0.48	-0.67	-0.17		0.24(0.07)
9.0	-0.87	-0.50	-0.68		-0.29	
9.6	-0.86	-0.52	-0.69	-0.20(0.2)		0.21(0.08)

pH	p_c[a]	p_a[b]	$E_{1/2}$[c]	$Fe^{II/Id}$	O_2 red[e]	$Fe^{III/IIf}$
10.0					-0.27	0.22
11.0	-1.05	-0.61	-0.83		-0.28	
12.2				-0.25(0)		-0.03(0.05)
12.5	-1.12	-0.71	-0.91		-0.33	
13.0	-1.13	-0.76	-0.95	-0.25(0)		-0.04(0.03)*
Zinc Data 2						
2.5	-0.22	-0.17	-0.20			
3.5	-0.30	-0.25	-0.28			
4.0	-0.35	-0.25	-0.30			
6.0	-0.45	-0.40	-0.43			
8.0	-0.62	-0.41	-0.52			
10.0	-0.68	-0.60	-0.64			
12.5	-0.88	-0.75	-0.82			
Cobalt Data 3						
2.0	-0.33	-0.32	-0.33		-0.20	
3.0	-0.49	-0.31	-0.40		-0.27	
4.0	-0.53	-0.45	-0.49		-0.32	
5.0	-0.66	-0.42	-0.54		-0.39	
6.0	-0.68	-0.55	-0.62		-0.56	
7.0	-0.77	-0.61	-0.69		-0.51	
8.0	-0.85	-0.63	-0.74		-0.54	
10.0	-1.08	-0.67	-0.88		-0.45	
12.0	-1.22	-0.85	-1.04		-0.47	

a) Cathodic peak potential for Pc(-2)/Pc(-3) anion reduction process; All data vs SCE, using cyclic voltammetry. b) Anodic peak potential for Pc(-2)/Pc(-3) anion reduction process; c) Average electrode potential for Pc(-2)/Pc(-3) anion reduction process; d) Proposed Fe(II)/Fe(I) couple, peak to peak separation in parenthesis; e) Oxygen reduction potential from peak of cyclic voltammogram under an oxygen atmosphere; f) Fe(III)/Fe(II) redox potential, peak to peak separation in parenthesis; g) All data were carried out on fresh surfaces except those with an asterisk which were all collected on the same surface,

Table 4. Variation of Redox Potentials (V) of Metal Phthalocyanine Redox Processes as a Function of Environment.[a]

Cobalt Species[b]	Conditions[c]	[MPc(-2)]/ [MPc(-3)][d]	[Co(II)Pc(-2)]/ [Co(I)Pc(-2)]⁻	Ref.
Cobalt				
CoTsPc/ads	Aq. pH 13	-1.37	-0.51	[44]
CoTsPc/ads	Aq. pH 2	-0.60	-0.31	[44]
CoTcPc/ads	1M H_2SO_4	-0.42	-0.27	[61]
CoTNPc/ads	Aq. pH 8		-0.71	tw
CoTNPc/ads	Aq. pH 4		-0.57	tw
CoTNPc	DCB[e]	-1.56	-0.40	[23]
CoCRPc/ads	Aq. pH 11		-0.60	[62]
CoCRPc/ads	Aq. pH 2	-0.48	-0.34	[62]
CoPc	Py		-0.61	[63]
CoPc/ads	Aq pH 14		-0.57	[64]
CoPc/ads	Aq pH 2		-0.29	[64]
Zinc				
ZnTNPc	DCB[e]	-1.15		[22]
ZnTNPc/ads	Aq pH 2	-0.48, -0.70		tw
ZnTNPc/ads	Aq pH 10	-1.13		tw
ZnPc	DMF	-0.86		[38]
ZnOBuPc	DMF	-1.06		[38]
ZnOCNPc	DMF	-0.15		[38]

Iron		[Fe(I)Pc(-2)]⁻ /[Fe(I)Pc(-3)]²⁻	Fe(II) /Fe(I)	Fe(III) /Fe(II)	Ref.
FeTsPc/ads	Aq pH 10.7	-1.17	-0.51	0.02	[56],tw
FeTsPc/ads	Aq pH 3.5	-0.55	-0.30	0.42	[56], tw
FePc/ads	Aq pH 14		-0.68	-0.26	[47][48]
FePc/ads	Aq pH 2			0.39	[47][48]
FePc	DMA	-1.17	-0.55	0.38	[32]

a) vs SCE. tw = this work. b) TsPc = tetrasulphonated phthalocyanine; also TNPc = tetraneopentoxyphthalocyanine; CRPc = tetracrownphthalocyanine; OBuPc = octabutoxyphthalocyanine; OCNPc = octacyanophthalocyanine.
ads = adsorbed on HOPG, or opg. c) DCB = o-dichlorobenzene, DMF = dimethylformamide, Py = pyridine, DMA = dimethylacetamide. d) M = Co(I) for cobalt complexes, and M = Zn(II) for zinc complexes. e) Referenced internally against ferrocenium/ferrocene couple assumed to lie at 0.51V vs SCE.

Table 5 - Solution Electrochemical Data for M[$Cl_{16}Pc$] in DMF

M	Electrolyte	$E_{1/2}$ (V vs. SCE)	Assignment	Method[a]
Fe[b]	TBA PF_6	0.73	$Fe(III)[Cl_{16}MPc(-2)]^+/Fe(II)[Cl_{16}Pc(-2)]$	DPV
		-1.11	$Fe(I)[Cl_{16}Pc(-2)]^-/Fe(I)[Cl_{16}Pc(-3)]^{2-}$	
		-1.73	$Fe(I)[Cl_{16}PcPc(-3)]^{2-}/Fe(I)[Cl_{16}PcPc(-4)]^{3-}$	
Co[b]	TBA PF_6	1.09	$Co(III)[Cl_{16}Pc(-2)]^+/Co(II)[Cl_{16}Pc(-2)]$	DPV
		-1.21	$Co(I)[Cl_{16}Pc(-2)]^-/Co(I)[Cl_{16}Pc(-3)]^{2-}$	
		-1.69	$Co(I)[Cl_{16}Pc(-3)]^{2-}/Co(I)[Cl_{16}Pc(-4)]^{3-}$	
Zn	LiCl/TBA PF_6	-0.5	$Zn[Cl_{16}Pc(-2)]/Zn[Cl_{16}Pc(-3)]^-$	CV
		-0.8	$Zn[Cl_{16}Pc(-3)]^-/Zn[Cl_{16}Pc(-4)]^{2-}$	

a) DPV = Differential Pulse Voltammetry; CV = Cyclic Voltammetry; b) These data were collected using a AgCl/Ag electrode and referenced internally to the Fc^+/Fc couple assumed to lie at 0.40V vs SCE in DMF.

c) TBA PF_6 = Tetra-Butyl Ammonium Hexafluorophosphate. Note that DPV peaks reported here do not correspond exactly with $E_{1/2}$ values.

Bibliography

1. Birchall, J.M.; Haszeldine, R.N.; Morley, J.O. J.Chem.Soc. (C), 1970, 2667-72.
2. Metz, J.; Schneider, O.; Hanack, M. Inorg.Chem., 1984, 23, 1065-71.
3. Yoshilke, N.; Kondo, S. Japan Patent JP 86/211849, 1986.
4. Takume, H.; Kuroda, S; Aiga, H. Japan Patent 86/308915, 1988.
5. Kuroiwa,A.; Nanba, N.; Kamijo, T. Japan Patent 86/24609, 1986.
6. Suzuki,T.; Murayama, T.; Ono, H.; Otsuka, S.; Nozomi, M. European Patent EP 180931, 1986.
7. Duggan, P.; Gordon, P.F. European Patent EP 155780, 1985.
8. Richo Co. Ltd. Japan Patent JP 88/60796, 1988.
9. Hung, Y.; Klosse, T.R.; Regan, M.T.; Rossi, L.J. Us Patent 4701396, 1987.
10. Sato, T. Japan Patent 86/162385, 1986.
11. Ricoh Co. Ltd. Japan Patent JP 83/56892, 1983.
12. Ricoh Co. Ltd. Japan Patent JP 83/112794, 1983.
13. Mandal, S.K.; Thompson, L.K.; Gabe, E.J.; Lee, F.L.; Charland, J-P. Inorg.Chem., 1987, 26, 2384-89.
14. Nevin, W.A.; Wei, L.. J.Anal.Spectry, 1988, 4, 559-63.
15. Janda, P.; Kobayashi, N.; Auburn, P.R. ; Lam, H.; Leznoff, C.C.; Lever, A.B.P. Can.J.Chem., 1988, 67, 1109-19.
16. Hempstead, M.R.; Lever, A.B.P.; Leznoff, C.C. Can.J.Chem., 1987, 65, 2677.
17. Lever, A.B.P.. J.Chem.Soc., 1965, 1821-29.
18. Barraclough, C.G.; Martin, R.L.; Mitra, S.; Sherwood, R.C. J.Chem.Phys., 1970, 53, 1643-48.
19. Dale, B.W.; Williams, R.J.P.; Johnson, C.E.; Throp, T.L. J.Chem.Phys., 1968, 49, 3441.
20. Martin, R.L.; Mitra, S. Chem.Phys.Let., 1969, 3, 183-4.
21. Gregson, A.K.; Martin, R.L.; Mitra, S. J.Chem.Soc. Dalton, 1976, 1458-66.

22. Manivannan, V.; Nevin, W.A.; Leznoff, C.C.; Lever, A.B.P.. J.Coord.CHem., 1988, 19, 139-58.

23. Nevin, W.A.; Hempstead, M.R.; Leznoff, C.C.; Lever, A.B.P.. Inorg.Chem., 1987, 26, 570-77.

24. Nevin, W.A.; Liu, W.; Melnik, M.; Lever, A.B.P. J.Electroanal.Chem., 1986, 213, 217-34.

25. Stillman, M.J.; Thompson, A.J. J.Chem.Soc. Far. II, 1974, 70, 790.

26. Dale, B.W. Trans. Far.Soc., 1969, 65, 331.

27. Kobayashi, N.; Nishigama, Y. J.Phys.Chem., 1985, 89, 1167.

28. Ercolani, C.; Gardini, M.; Murray, K.S.; Pennesi, G.; Rossi, G. Inorg.Chem., 1987, 25, 3927.

29. Ercolani, C.;Rossi, G.; Montanelli, F. Inorg.Chim.Acta, 1980, 44, L215.

30. Ercolani, C.; Gardini, M.; Pennesi, G.; Rossi, G.. Inorg.Chem., 1983, 22, 2534.

31. Lever, A.B.P.; Licoccia, S.; Ramaswamy, B.S. Inorg.Chim.Acta, 1982, 64, L87.

32. Lever, A.B.P.; Wilshire, J.P. Inorg.Chem., 1978, 17, 1145-51.

33. Clack, D.W.; Yandle, J.R.. Inorg.Chem., 1972, 11, 1738.

34. Myers, J.F.; Rayner-Canham, G.W.; Lever, A.B.P. Inorg.Chem., 1975, 14, 461-8.

35. Nevin, W.A.; Wei, L.; Lever, A.B.P. Can.J.Chem., 1987, 65, 855-58.

36. Nevin, W.A.; Hempstead, R.H.; Wei, L.; Leznoff, C.C.; Lever, A.B.P.. Inorg.Chem., 1987, 26, 570-77.

37. Minor, P.C.; Gouterman, M.; Lever, A.B.P. Inorg.Chem., 1985, 24, 1894-1900.

38. Wohrle, D.; Schmidt, V. J.Chem.Soc. Dalton, 1988, 549-51.

39. Wohrle, D.; Schulte, B. Makromol.Chem., 1988, 189, 1167-87.

40. Forster, T. Naturwiss., 1949, 36, 186.

41. Weller, A. Prog.React.Kin., 1961, 1, 189-214.

42. Hale, P.D.; Pietro, W.J.; Ratner, M.A.; Ellis, D.E.; Marks, T.J. J.Am.Chem.Soc., 1987, 109, 5943-47.

43. Gaspard, S.; Verdaguer, M.; Viovy, R. J.Chem.Res. (S), 1979, 271-74.

44. Zecevic, Z.; Simic-Glavaski, B.; Yeager, E.; ; Lever, A.B.P.; Minor, P.C. J.Electroanal.Chem., 1985, 196, 339-358.

45. Elzing, A.; Van der Putten, A.; Visscher, W.; Barendrecht, E.. J.Electroanal.Chem., 1986, 200, 313.

46. Van der Putten, A.; Elzing, A.; Visscher, W.; Barendrecht, E.. J.Electroanal.Chem., 1987, 233, 113.

47. Van der Putten, A.; Elzing, A.; Visscher, W.; Barendrecht, E. J.Electroanal.Chem., 1986, 214, 523.

48. Van der Putten, A.; Elzing, A.; Visscher, W.; Barendrecht, E. J.Electroanal.Chem., 1987, 221, 95.

49. Lever, A.B.P.; Minor, P.C. Inorg.Chem., 1981, 20, 4015-17.

50. Clack, D.W.; Hush, N.S.; Woolsey, I.S. Inorg.Chim.Acta, 1976, 19, 129-32.

51. Van Den Brink, F.; Visscher, W.; Barendrecht, E.. J.Electroanal.Chem., 1983, 157, 283-304.

52. Van Veen, J.A.R.; Visser, C. Electrochimica Acta, 1979, 24, 921-8.

53. Van den Brink, F.; Barendrecht, E.; Visscher, W. Rec.Trav.Chim.Pays Bas., 1980, 99, 253.

54. Appleby, A.J.; Savy, M.. Electrochimica Acta, 1976, 21,

55. Appleby, A.J.; Fleisch, J.; Savy, M.. J.Catal., 1976, 44, 281.

56. Zagal, J.; Bindra, P.; Yeager, E. . J.Electroanal.Chem., 1980, 127, 1506.

57. Zagal, J.; Sen, R.K.; Yeager, E.. J.Electroanal.Chem., 1977, 83, 207.

58. Appleby, A.J.; Caro, P.; Savy, M.. J.Electroanal.Chem., 1980, 111, 91-96.

59. Achar, B.N.; Fohlen, G.M.; Parker, J.A.; Keshavayya, J. Polyhedron, 1987, 6, 1463-67.

60. Freyer, W. Z.Chem., 1986, 26, 216-7.

61. Kusuda, K.; Shiraki, K.; Yamaguchi, H. Ber.Bunsen Phys.Chem., 1988, 92, 725-30.

62. Kobayashi, N.; Lever, A.B.P.. J.Am.Chem.Soc., 1987, 109, 7433-41.

63. Lever, A.B.P.; Wilshire, J.P. Can.J.Chem., 1976, 54, 2514-16.

64. Van Den Putten, A. Ph.D. Thesis, Amsterdam, 1986,

Scheme 1.

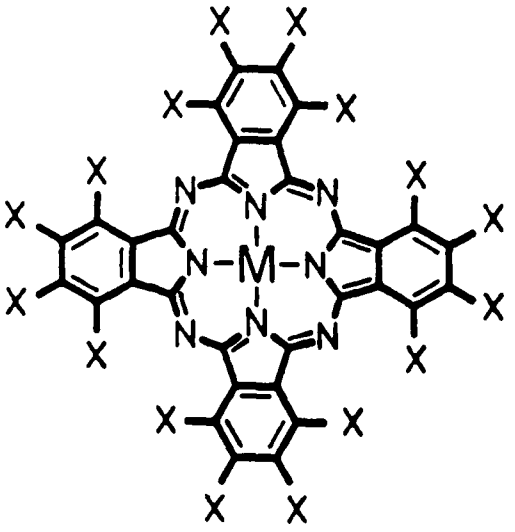

X = H MPc

X = Cl M = Fe 1

X = Cl M = Zn 2

X = Cl M = Co 3

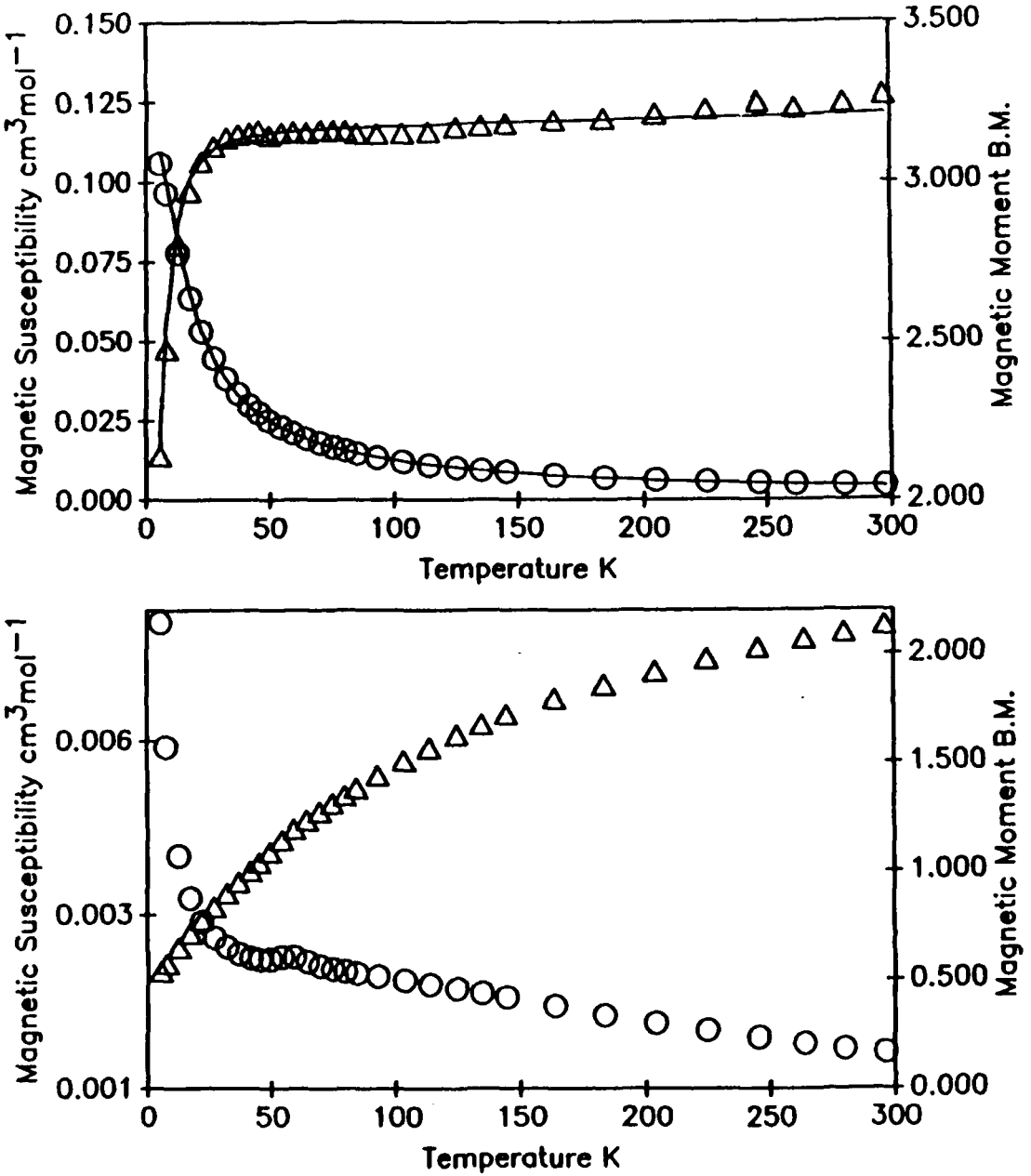
0.150
0.125
0.100
0.075
0.050
0.025
0.000
Magnetic Susceptibility cm^{3}mol^{-1}
3.500
3.000
2.500
2.000
Magnetic Moment B.M.
0
50
100
150
200
250
300
Temperature K
0.006
0.003
0.001
Magnetic Susceptibility cm^{3}mol^{-1}
2.000
1.500
1.000
0.500
0.000
Magnetic Moment B.M.
0
50
100
150
200
250
300
Temperature K

2

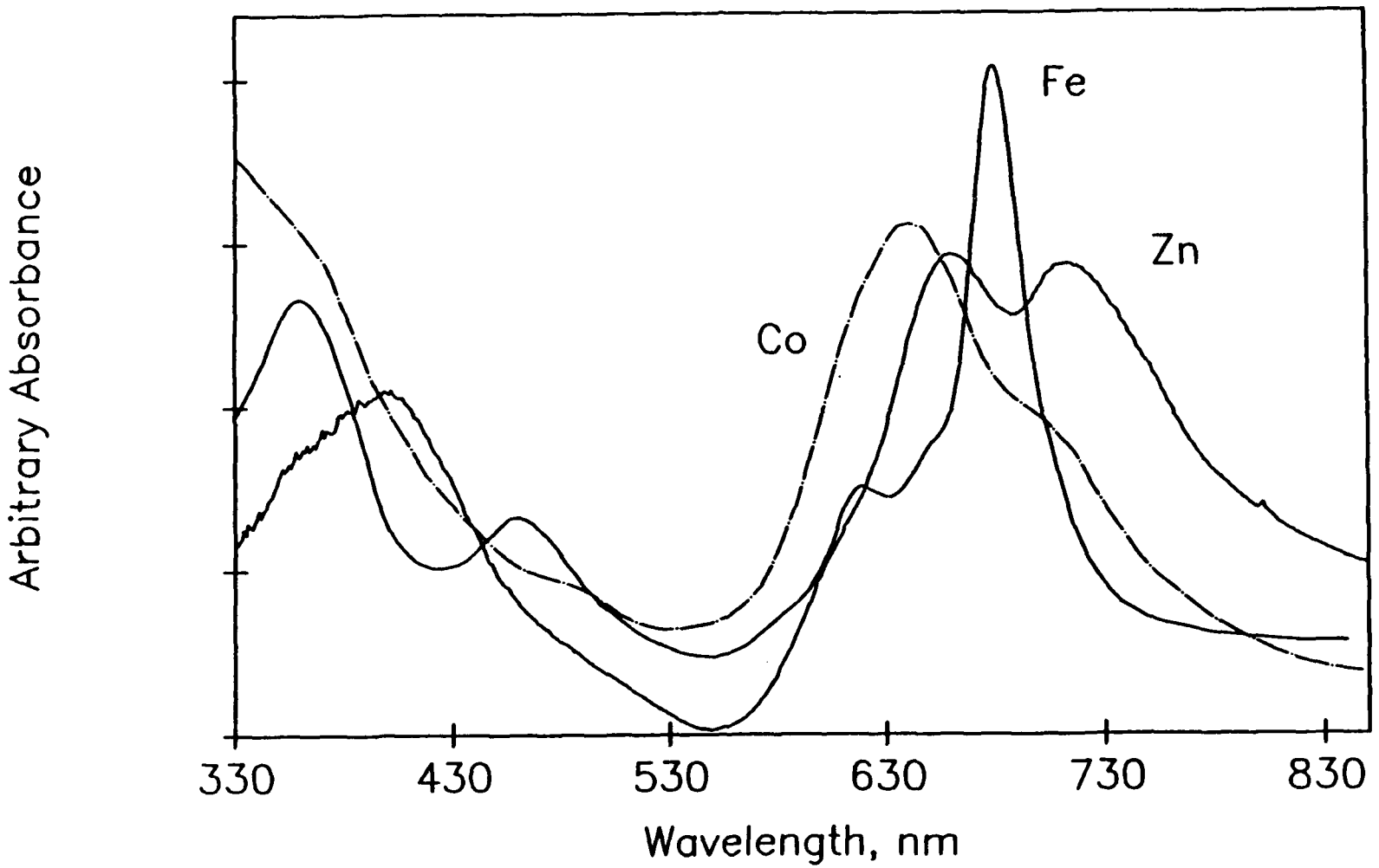
Arbitrary Absorbance
Fe
Zn
Co
330
430
530
630
730
830
Wavelength, nm

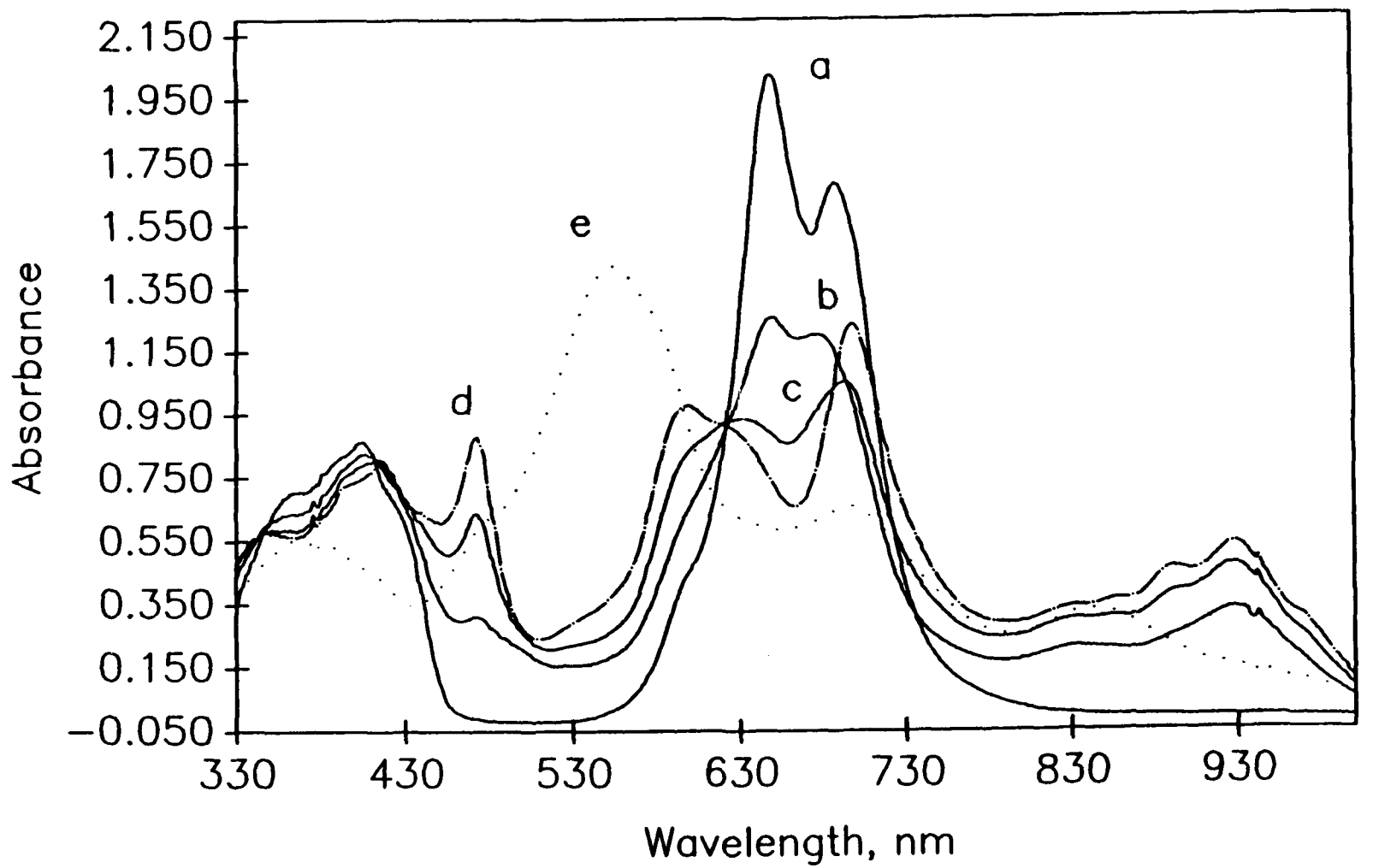
2.150
1.950
1.750
1.550
1.350
1.150
0.950
0.750
0.550
0.350
0.150
−0.050
Absorbance
330
430
530
630
730
830
930
Wavelength, nm
a
b
c
d
e

4

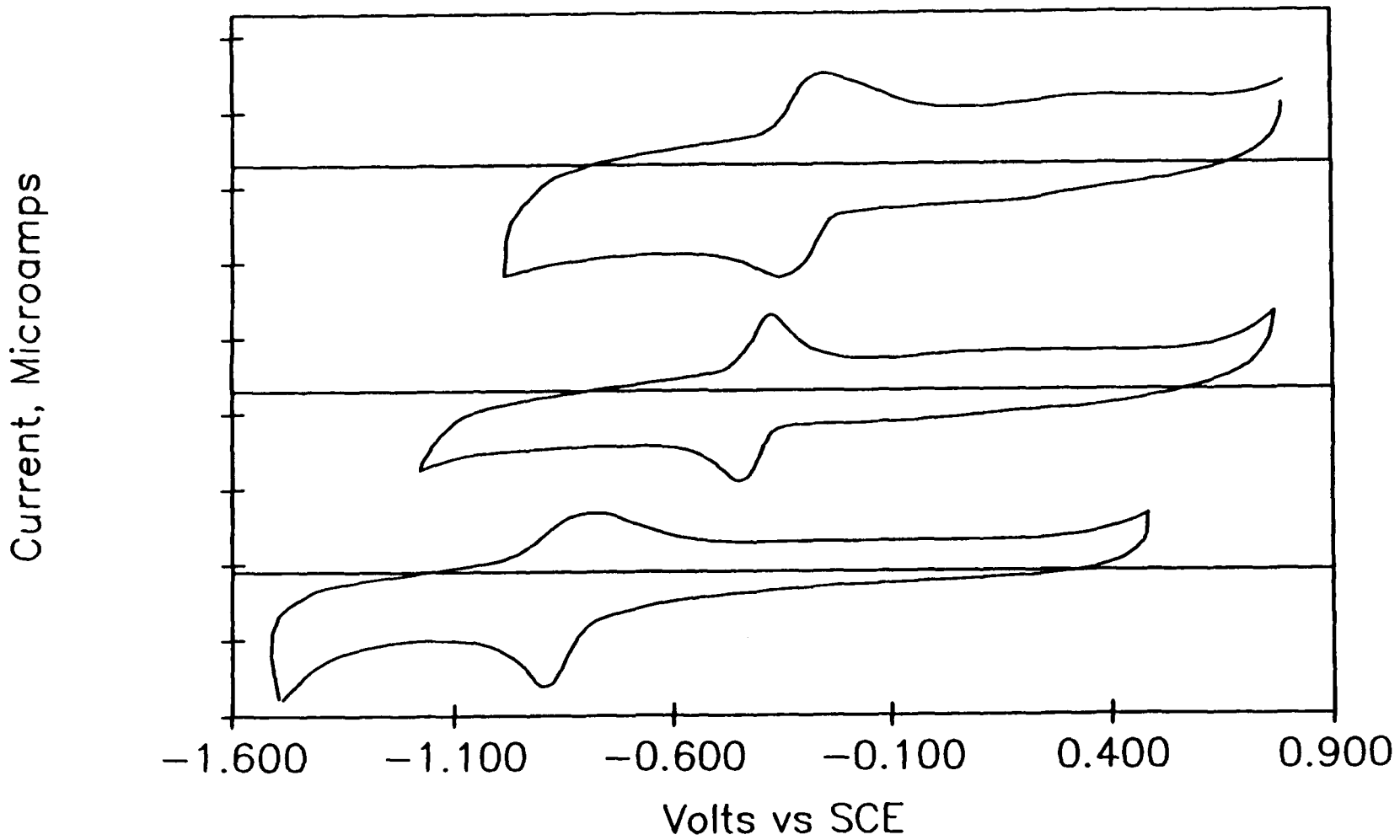
Current, Microamps
−1.600
−1.100
−0.600
−0.100
0.400
0.900
Volts vs SCE

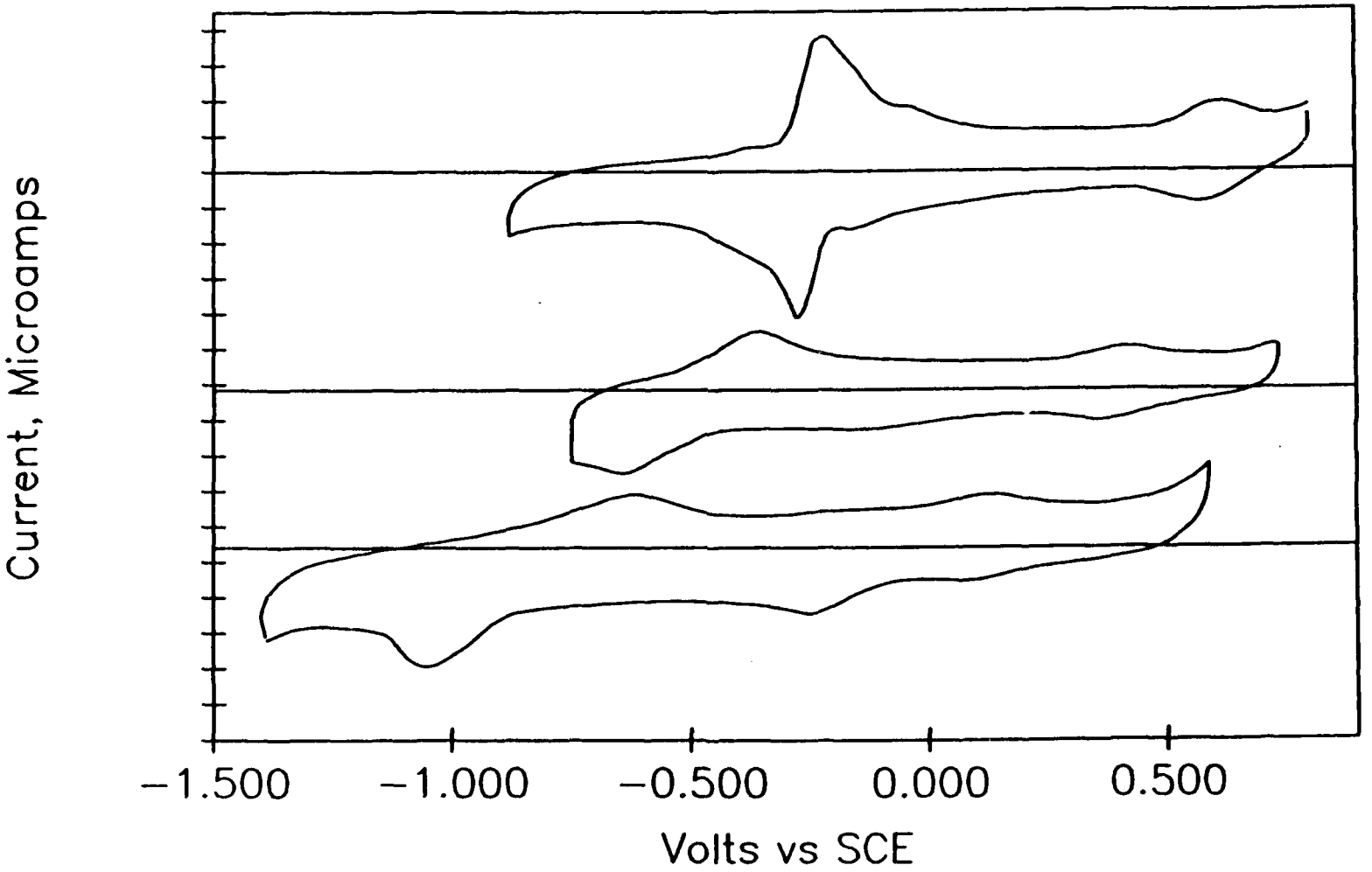
Current, Microamps
−1.500
−1.000
−0.500
0.000
0.500
Volts vs SCE

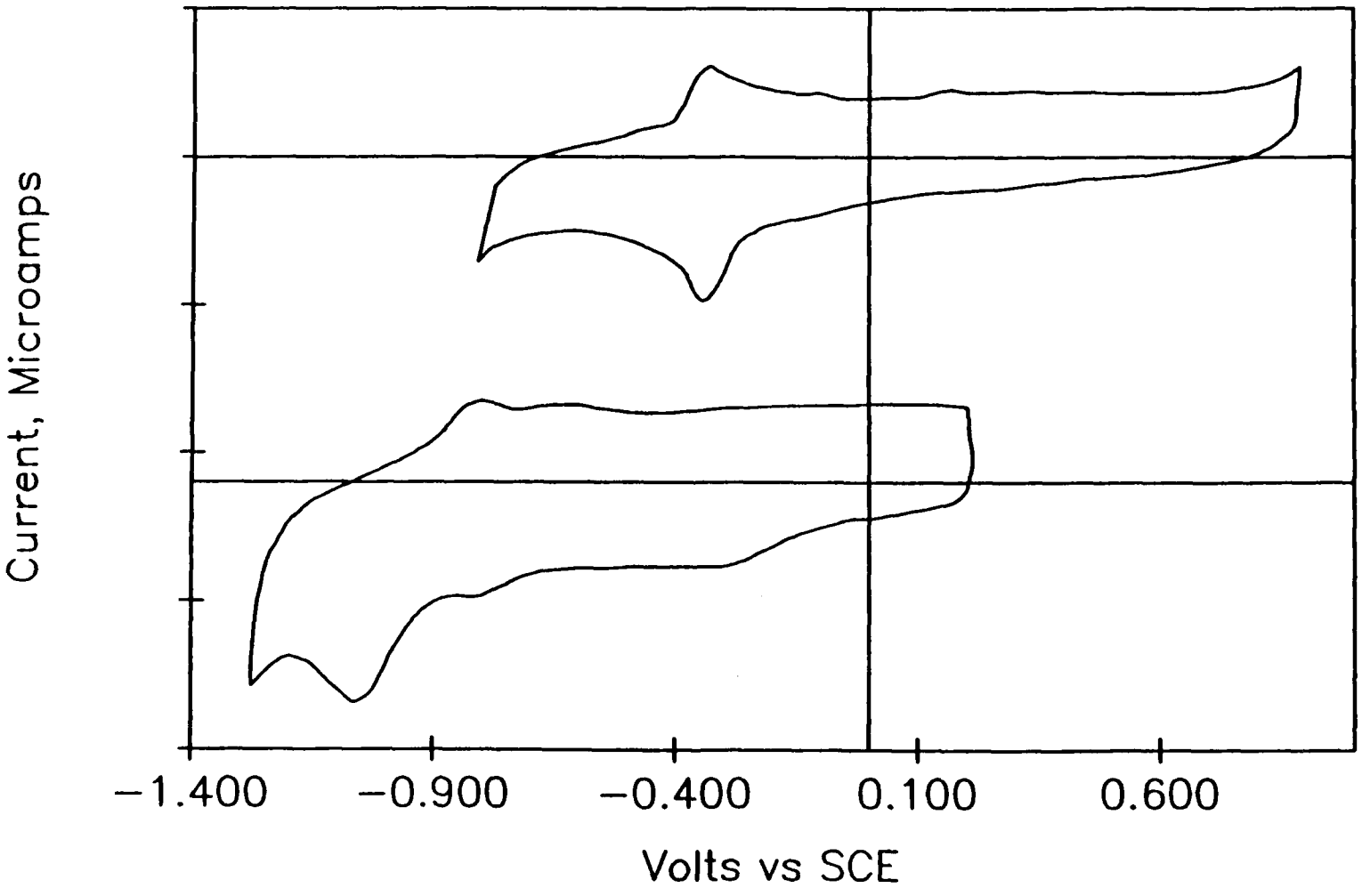
Current, Microamps
−1.400
−0.900
−0.400
0.100
0.600
Volts vs SCE

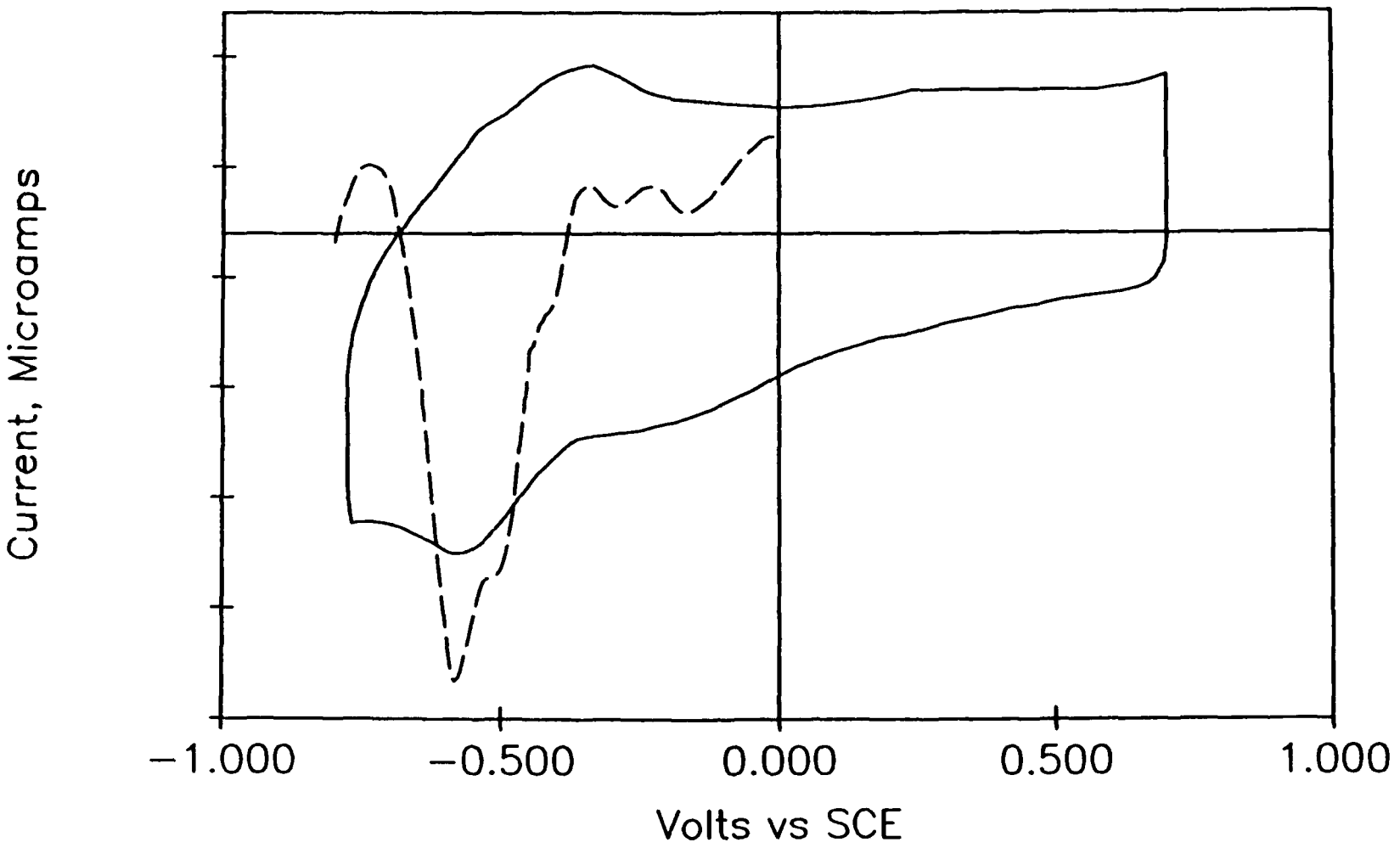
Current, Microamps
−1.000
−0.500
0.000
0.500
1.000
Volts vs SCE

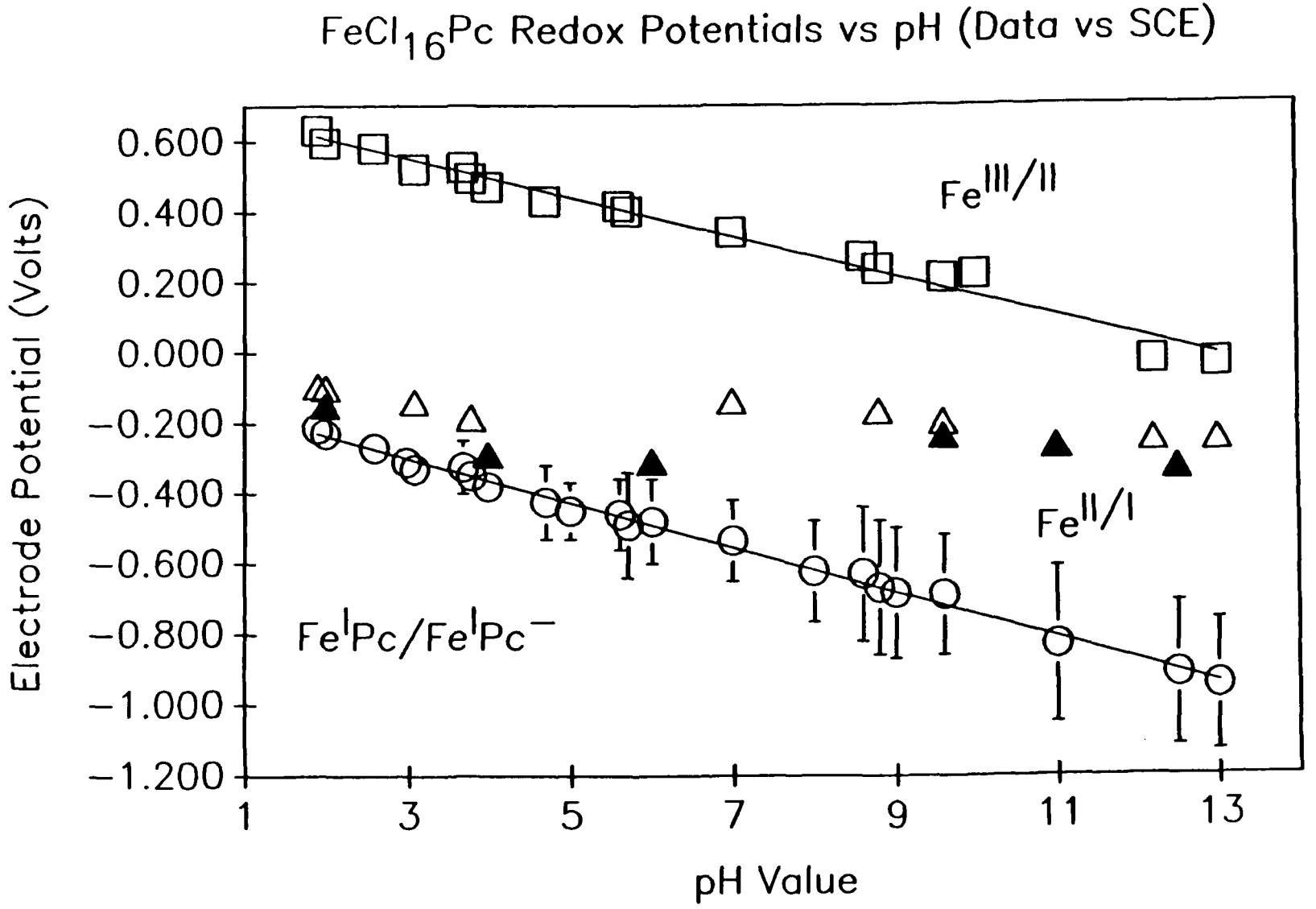
FeCl16Pc Redox Potentials vs pH (Data vs SCE)
Electrode Potential (Volts)
0.600
0.400
0.200
0.000
−0.200
−0.400
−0.600
−0.800
−1.000
−1.200
1
3
5
7
9
11
13
pH Value
Fe III/II
Fe II/I
Fe I Pc/Fe I Pc−

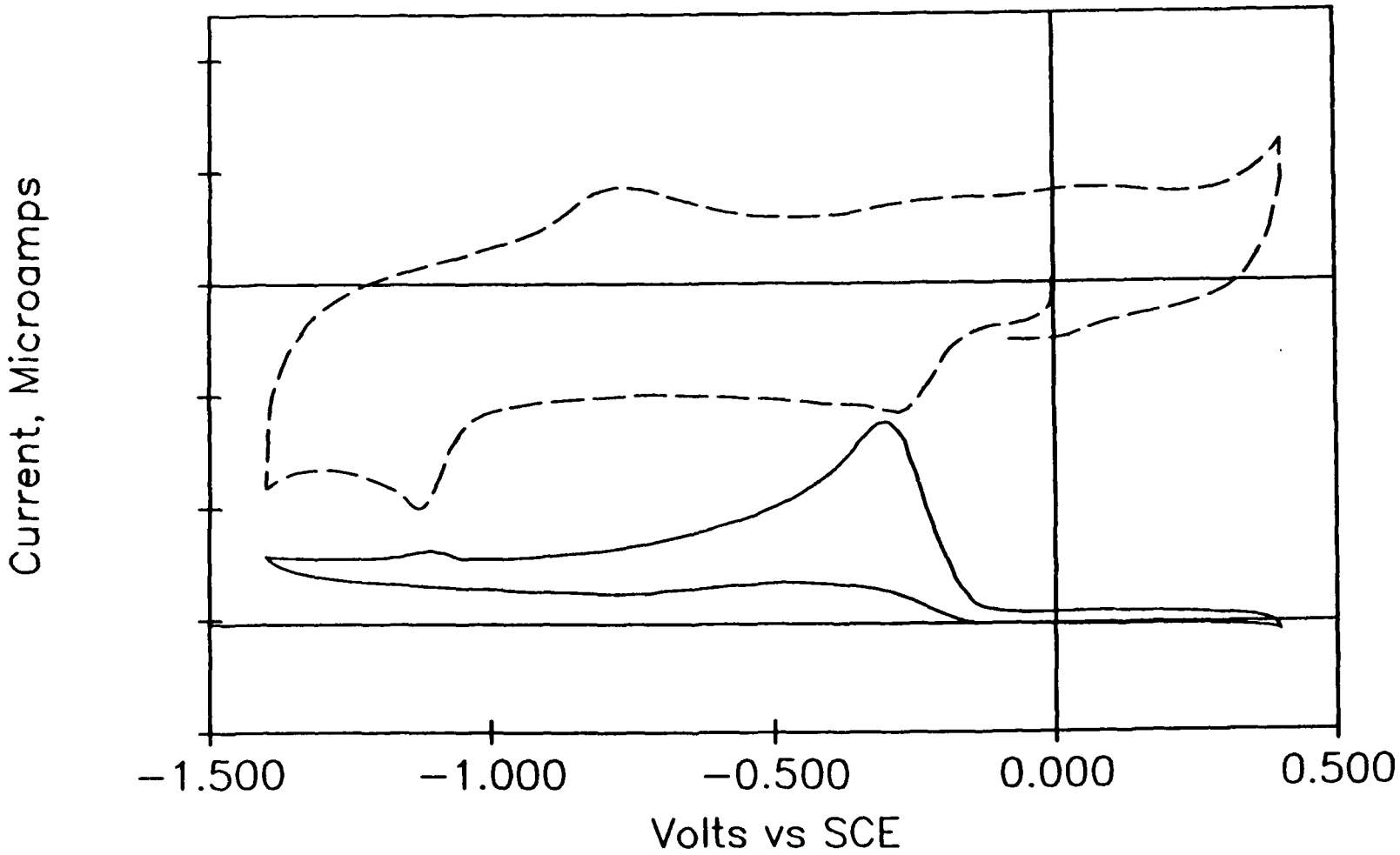
Current, Microamps
−1.500
−1.000
−0.500
0.000
0.500
Volts vs SCE